Dalton Transactions

ROYAL SOCIETY OF CHEMISTRY

PAPER

View Article Online
View Journal | View Issue

Cite this: *Dalton Trans.*, 2020, **49**, 210

Half-sandwich ruthenium(II) complexes with tethered arene-phosphinite ligands: synthesis, structure and application in catalytic cross dehydrogenative coupling reactions of silanes and alcohols†

Rebeca González-Fernández, Pascale Crochet * and Victorio Cadierno *

The preparation of the tethered arene-ruthenium(II) complexes [$RuCl_2\{\eta^6{:}\kappa^1(P)\text{-}C_6H_5(CH_2)_nOPR_2\}$] (R = Ph, n = 1 (**9a**), 2 (**9b**), 3 (**9c**); R = ^{i}Pr, n = 1 (**10a**), 2 (**10b**), 3 (**10c**)) from the corresponding phosphinite ligands $R_2PO(CH_2)_nPh$ (R = Ph, n = 1 (**1a**), 2 (**1b**), 3 (**1c**); R = ^{i}Pr, n = 1 (**2a**), 2 (**2b**), 3 (**2c**)) is presented. Thus, in a first step, the treatment at room temperature of tetrahydrofuran solutions of dimers [{RuCl(μ-Cl)(η^6-arene)}$_2$] (arene = *p*-cymene (**3**), benzene (**4**)) with **1-2a-c** led to the clean formation of the corresponding mononuclear derivatives [$RuCl_2(\eta^6\text{-}p\text{-cymene})\{R_2PO(CH_2)_nPh\}$] (**5-6a-c**) and [$RuCl_2(\eta^6\text{-benzene})\{R_2PO(CH_2)_nPh\}$] (**7-8a-c**), which were isolated in 66–99% yield. The subsequent heating of 1,2-dichloroethane solutions of these compounds at 120 °C allowed the exchange of the coordinated arene. The substitution process proceeded faster with the benzene derivatives **7-8a-c**, from which complexes **9-10a-c** were generated in 61–82% yield after 0.5–10 h of heating. The molecular structures of [$RuCl_2(\eta^6\text{-}p\text{-cymene})\{^iPr_2PO(CH_2)_3Ph\}$] (**6c**) and [$RuCl_2\{\eta^6{:}\kappa^1(P)\text{-}C_6H_5(CH_2)_nOP^iPr_2\}$] ($n$ = 1 (**10a**), 2 (**10b**), 3 (**10c**)) were unequivocally confirmed by X-ray diffraction methods. In addition, complexes [$RuCl_2\{\eta^6{:}\kappa^1(P)\text{-}C_6H_5(CH_2)_nOPR_2\}$] (**9-10a-c**) proved to be active catalysts for the dehydrogenative coupling of hydrosilanes and alcohols under mild conditions (r.t.). The best results were obtained with [$RuCl_2\{\eta^6{:}\kappa^1(P)\text{-}C_6H_5(CH_2)_3OP^iPr_2\}$] (**10c**), which reached TOF and TON values up to 117 600 h^{-1} and 57 000, respectively.

Received 15th November 2019,
Accepted 2nd December 2019

DOI: 10.1039/c9dt04421c

rsc.li/dalton

Introduction

Since the pioneering work of Winkhaus and Singer in 1967,[1] the chemistry of half-sandwich (η^6-arene)-ruthenium(II) complexes has exponentially expanded, representing nowadays one of the most versatile and widely studied families of organometallic ruthenium complexes.[2] Relevant applications of this type of compounds in catalysis,[3] biomedicine[4] and supramolecular chemistry[5] have been described during the last two decades. A special subset of (η^6-arene)-ruthenium(II) complexes are the so-called tethered derivatives (Fig. 1), in which the η^6-coordinated arene ligand is linked to a pendant donor atom which also coordinates to the metal center (polydentate examples involving two or three σ-donor units are obviously known).[6] In comparison with their non-tethered counterparts, these complexes gain robustness and rigidity from the chelate effect, which has found to be advantageous in the field of homogeneous catalysis as they can be used at higher temperatures, over prolonged reaction periods, and also because they allow a better stereodiscrimination in asymmetric processes.[7]

A large number of tethered arene-ruthenium(II) complexes featuring C-,[8] N-,[9] O-,[10] S-,[11] As-,[12] and P-donor[6,13] units are currently known, with the latter being by far the most numer-

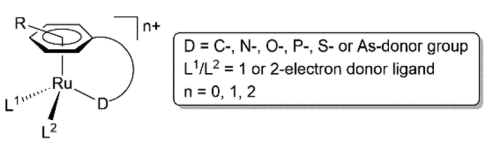

Fig. 1 Generic structure of tethered arene-ruthenium(II) complexes.

Laboratorio de Compuestos Organometálicos y Catálisis (Unidad Asociada al CSIC), Centro de Innovación en Química Avanzada (ORFEO-CINQA), Departamento de Química Orgánica e Inorgánica, Instituto Universitario de Química Organometálica "Enrique Moles", Facultad de Química, Universidad de Oviedo, Julián Clavería 8, E-33006 Oviedo, Spain. E-mail: crochetpascale@uniovi.es, vcm@uniovi.es; Fax: +(34)985103446; Tel: +(34) 985103453

†Electronic supplementary information (ESI) available: Copies of the NMR spectra of all the ruthenium complexes synthesized in this work and the alkoxysilanes isolated in the catalytic experiments. Kinetic profile of the dehydrogenative cross-coupling reaction of Me_2PhSiH with MeOH catalyzed by 0.005 mol% of **10c**. CCDC 1958494 (**6c**), 1958495 (**10a**), 1958496 (**10b**) and 1958497 (**10c**). For ESI and crystallographic data in CIF or other electronic format see DOI: 10.1039/c9dt04421c

ous. However, the vast majority of examples involves phosphine-type ligands, typically containing two- or three carbon spacers connecting the phosphorus atom and the arene group.[6,13] The use of other phosphorus donors remains almost unexplored. In this regard, complexes **A**,[14] **B**[15] and **C**[16] are the only ruthenium(II) complexes incorporating η^6-arene-κ^1-phosphinite ligands quoted to date in the literature (see Fig. 2).[17–19] Interestingly, while the synthesis of complexes **A** and **B** was accomplished in two steps from the corresponding phosphinite ligand and appropriate dimeric precursor, *i.e.* [{RuCl(μ-Cl)(η^6-$C_6H_5CO_2Me$)}$_2$] or [{RuCl(μ-Cl)(η^6-*p*-cymene)}$_2$], *via* initial cleavage of the chloride bridges by the phosphinite and subsequent intramolecular exchange of the arene on the resulting κ^1-(*P*) mononuclear adducts,[14,15] compounds [$RuCl_2\{\eta^6$:$\kappa^1(P)$-$C_6H_5CH_2CH_2CH_2OPR_2\}$] (**C**) were generated in modest yield (25–44%) by reacting the 3-phenylpropanol-ruthenium(II) derivative [$RuCl_2\{\eta^6$:$\kappa^1(O)$-$C_6H_5CH_2CH_2CH_2OH\}$] with the corresponding chlorophosphine R_2PCl in the presence of base.[17,20]

In this contribution, an alternative and more efficient synthesis of complexes **C**, as well as that of related species containing shorter carbon spacers between the oxygen atom and the phenyl group, *i.e.* compounds [$RuCl_2\{\eta^6$:$\kappa^1(P)$-$C_6H_5CH_2CH_2OPR_2\}$] and [$RuCl_2\{\eta^6$:$\kappa^1(P)$-$C_6H_5CH_2CH_2OPR_2\}$] (R = Ph, ^{i}Pr), is presented employing the preformed phosphinites as starting materials. In addition, all the tethered complexes were evaluated as potential catalysts for the dehydrogenative cross-coupling of hydrosilanes with alcohols, showing excellent activities under mild conditions.[21]

Results and discussion

Our investigations started with the preparation of the phosphinite ligands $Ph_2PO(CH_2)_nPh$ (*n* = 1 (**1a**), 2 (**1b**), 3 (**1c**)) and $^iPr_2PO(CH_2)_nPh$ (*n* = 1 (**2a**), 2 (**2b**), 3 (**2c**)). They were obtained in 50–77% yield by following the route described by Mukaiyama and co-workers,[22] based on the initial deprotonation of the corresponding primary alcohol with ^{n}BuLi in tetrahydrofuran, and subsequent addition of chlorodiphenylphosphine or chlorodiisopropylphosphine to the resulting alcoholate solution (Scheme 1).

With compounds $R_2PO(CH_2)_nPh$ (**1-2a-c**) in hands, we next explored their coordination to ruthenium. In particular, we initially synthesized the mononuclear complexes [$RuCl_2$(η^6-*p*-cymene){$R_2PO(CH_2)_nPh$}] (**5-6a-c**) and [$RuCl_2$(η^6-benzene){$R_2PO(CH_2)_nPh$}] (**7-8a-c**), featuring a κ^1-(*P*) coordination of the ligands,[23] by treatment of the corresponding dimeric precursor [{RuCl(μ-Cl)(η^6-arene)}$_2$] (arene = *p*-cymene (**3**), benzene (**4**))[24] with 2.7 equivalents of **1-2a-c** (Scheme 2). The reactions, which were performed in tetrahydrofuran at room temperature, afforded **5-8a-c** as air-stable orange solids in 66–90% yield. As a consequence of the lower solubility of dimer [{RuCl(μ-Cl)(η^6-benzene)}$_2$] (**4**) in THF with respect to its *p*-cymene analogue **3**, longer reaction times were systematically required in the syntheses of the benzene derivatives **7-8a-c** (12 h *vs.* 1 h in the case of **5-6a-c**).

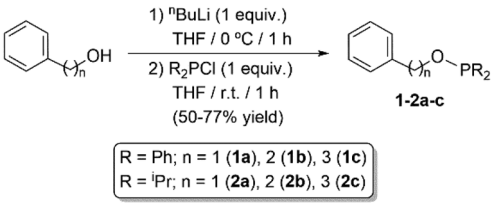

Scheme 1 Synthesis of the phosphinite ligands $R_2PO(CH_2)_nPh$ (**1-2a-c**).

As expected, the formation of all these complexes could be conveniently monitored by $^{31}P\{^1H\}$ NMR spectroscopy, the spectra showing a slight shift of the phosphorus signal to high fields ($\Delta\delta$ from −1.1 to −3.6 ppm) in comparison to the corresponding uncoordinated $R_2PO(CH_2)_nPh$ ligand (see Table 1). The ^1H and $^{13}C\{^1H\}$ NMR spectra obtained also exhibited signals in accordance with the proposed formulations, and satisfactory elemental analyses were in all the cases obtained (see details in the Experimental section).

In addition, single crystals of [$RuCl_2$(η^6-*p*-cymene){$^iPr_2PO(CH_2)_3Ph$}] (**6c**) suitable for X-ray diffraction analysis could be obtained by slow diffusion of *n*-hexane into a saturated solution of the complex in tetrahydrofuran, thus allowing to unequivocally confirm the structures proposed for **5-8a-c**. An ORTEP-type view of the molecule is shown in Fig. 3 along with selected bonding parameters. The complex features a typical three-legged piano-stool geometry, with the ruthenium atom surrounded by the η^6-bonded *p*-cymene ring, two chlorides, and the phosphorus atom of the phosphinite ligand. The Ru–Cl bond lengths (2.404(1) and 2.410(1) Å) and Cl(1)–Ru–Cl(2) angle (85.83(2)°) fall within the expected range for [$RuCl_2$(η^6-*p*-

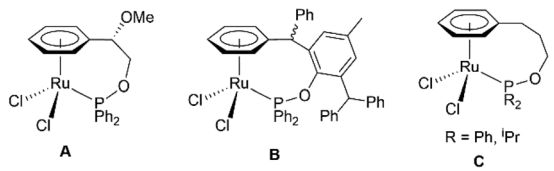

Fig. 2 Structure of the η^6-arene-κ^1-phosphinite-ruthenium(II) complexes **A**–**C**.

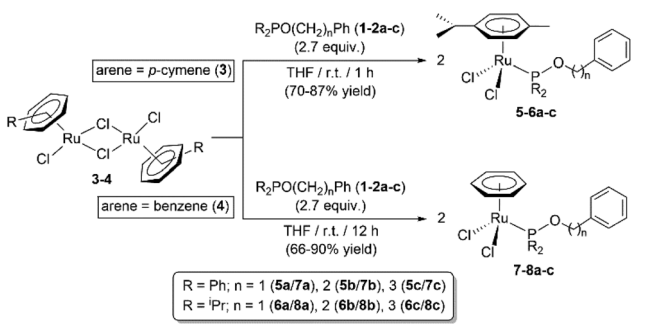

Scheme 2 Synthesis of the arene-ruthenium(II) complexes **5-8a-c**.

Table 1 $^{31}P\{^1H\}$ NMR data for the phosphinite ligands **1-2a-c** and the ruthenium(II) complexes **5-10a-c** [a]

Comp.	δ_P	Comp.	δ_P	Comp.	δ_P	Comp.	δ_P
1a	114.5	**5a**	111.6	**7a**	111.2	**9a**	158.6
1b	112.6	**5b** [b]	110.1	**7b**	109.0	**9b**	121.5
1c	112.1	**5c** [b]	109.5	**7c**	109.3	**9c** [b]	119.3
2a	154.5	**6a**	151.9	**8a**	150.9	**10a**	206.2
2b	152.2	**6b**	150.7	**8b**	148.5	**10b**	159.8
2c	151.4	**6c**	150.3	**8c**	148.0	**10c**	156.3

[a] Unless otherwise stated, the spectra were recorded in $CDCl_3$ at r.t. δ_P in ppm. [b] Spectra recorded in CD_2Cl_2 at r.t.

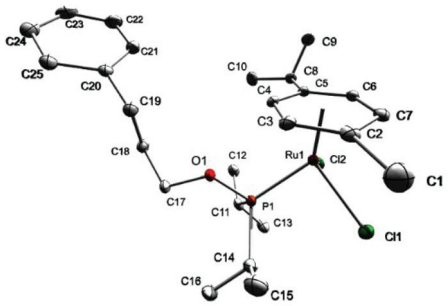

Fig. 3 ORTEP-type view of the structure of complex **6c** showing the crystallographic labelling scheme. Hydrogen atoms have been omitted for clarity. Thermal ellipsoids are drawn at the 30% probability level. Selected bond distances (Å) and angles (°): Ru–C* = 1.712(2); Ru–Cl(1) = 2.404(1); Ru–Cl(2) = 2.410(1); Ru–P(1) = 2.351(1); P(1)–O(1) = 1.619(2); P(1)–C(11) = 1.839(2); P(1)–C(14) = 1.850(1); O(1)–C(17) = 1.452(2); C*–Ru–P(1) = 126.78(2); C*–Ru–Cl(1) = 124.95(2); C*–Ru–Cl(2) = 124.43(1); Cl(1)–Ru–Cl(2) = 85.83(2); Cl(1)–Ru–P(1) = 90.01(2); Cl(2)–Ru–P(1) = 93.21(2); Ru–P(1)–O(1) = 105.28(5); Ru–P(1)–C(11) = 121.12(7); Ru–P(1)–C(14) = 114.88(7); C(11)–P(1)–C(14) = 103.60(9); C(11)–P(1)–O(1) = 104.15(9); C(14)–P(1)–O(1) = 106.57(9); P(1)–O(1)–C(17) = 127.5(1); C* denotes the centroid of the *p*-cymene unit (C(2), C(3), C(4), C(5), C(6) and C(7)).

cymene)(PR_3)]-type complexes, and the Ru–P(1) and P(1)–O(1) distances (2.351(1) and 1.619(2) Å, respectively) are comparable to those recently found by Balakrishna and co-workers in the solid-state crystal structure of the related phosphinite-ruthenium(II) derivative $[RuCl_2(\eta^6$-*p*-cymene)$(Ph_2POCH_2CH_2\{1,2,3\text{-}N_3C(Ph)C(H)\})]$ (Ru–P = 2.301(1) Å and P–O = 1.615(2) Å).[25]

Complexes **5-8a-c** were found to be perfectly stable in solution at room temperature for long periods, not observing, regardless of the solvent employed, the displacement of the *p*-cymene or benzene ligands. In the search of suitable experimental conditions for the generation of the corresponding tethered complexes, we performed a series of experiments with CH_2Cl_2, tetrahydrofuran, 1,2-dichloroethane and toluene solutions of $[RuCl_2(\eta^6$-*p*-cymene$)\{Ph_2PO(CH_2)_nPh\}]$ (**5a–c**) at different temperatures. We could only observe the selective formation of the desired complexes $[RuCl_2\{\eta^6{:}\kappa^1(P)\text{-}C_6H_5(CH_2)_nOPPh_2\}]$ (**9a–c**) working in 1,2-dichloroethane (DCE) at 120 °C (reactions performed in a sealed tube).[26] However, the conversions were very low (≤30%) even after 48 h of heating. To our delight, employing the same experimental conditions, the more labile character of the Ru-benzene *vs.* Ru-cymene bond[24,27] allowed the high yield preparation of compounds **9a–c** from $[RuCl_2(\eta^6$-benzene$)\{Ph_2PO(CH_2)_nPh\}]$ (**7a–c**) (Scheme 3). Interestingly, the reactions times needed for the complete consumption of the starting materials were found to be strongly influenced by the number of carbon atoms connecting the phosphinite and phenyl units, with a time increasing with the spacer's length (from 2 h for **7a** to 10 h for **7c**).

Concerning the preparation of their diisopropylphosphinite counterparts, *i.e.* compounds $[RuCl_2\{\eta^6{:}\kappa^1(P)\text{-}C_6H_5(CH_2)_nOP^iPr_2\}]$ (**10a–c**), we found that they can be conveniently accessed employing both $[RuCl_2(\eta^6$-*p*-cymene$)\{^iPr_2PO(CH_2)_nPh\}]$ (**6a–c**) and $[RuCl_2(\eta^6$-benzene$)\{^iPr_2PO(CH_2)_nPh\}]$ (**8a–c**) as starting materials, with only minor differences in yields and reaction times between them (see Scheme 4). The greater reactivity of these derivatives in comparison to that of compounds **5a–c** and **7a–c** can be ascribed to the higher electron density of the metal center, which labilizes the ruthenium–arene bond through back-donation from the occupied d ruthenium orbitals to the empty π* arene ones.[28] On the other hand, although to a lesser extent, the effect of the length of the spacer on the reaction rates was also observed in these cases. The $\eta^6{:}\kappa^1(P)$-coordination of the phosphinite ligands was reflected in the $^{31}P\{^1H\}$ NMR spectra of complexes **9-10a-c** by a downfield shift of the phosphorus signals with respect to those of their non-tethered precursors ($\Delta\delta$ = 6–56 ppm; see Table 1). The greatest deshielding effect was observed for $[RuCl_2\{\eta^6{:}\kappa^1(P)\text{-}C_6H_5CH_2OPR_2\}]$ (R = Ph (**9a**), ^{i}Pr (**10a**)), which according to the X-ray data (see below) contain the more strained chelate ring.[29] The ^1H NMR spectra of **9-10a-c** confirmed the coordination of the pendant phenyl unit of the phosphinite ligands to ruthenium, displaying three well-separated signals: two triplets at δ_H 6.15–6.49 and 5.76–6.12 ppm and one doublet at δ_H 5.09–5.54 ppm with integrated intensities of 1 : 2 : 2 and mutual $^3J_{HH}$ coupling constants of 4.5–6.0 Hz, assigned to the

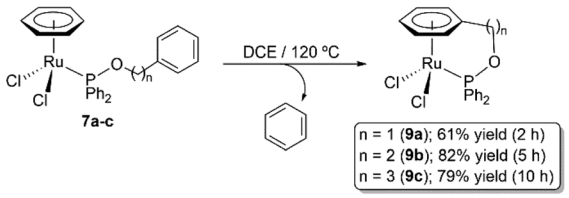

Scheme 3 Synthesis of the tethered arene-ruthenium(II) complexes **9a–c**.

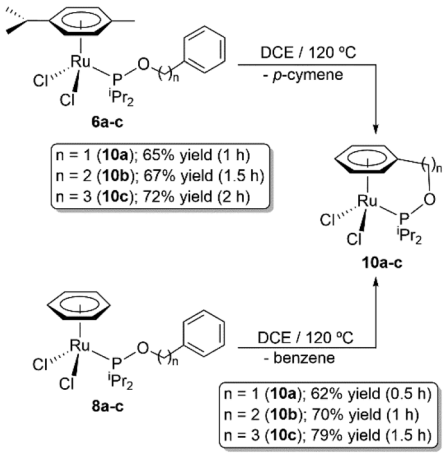

Scheme 4 Synthesis of the tethered arene-ruthenium(II) complexes **10a–c**.

para, *meta* and *ortho* protons, respectively. The chemical equivalence of the *ortho* and *meta* carbons was also evidenced in the $^{13}C\{^1H\}$ NMR spectra, which featured in all the cases four signals for the η^6-coordinated phenyl group in the δ_C range 84.5–108.8 ppm (see details in the Experimental section).

To confirm the spectroscopic information and to have a better insight into the structure of the complexes synthesized, X-ray diffraction studies were carried out on $[RuCl_2\{\eta^6{:}\kappa^1(P)\text{-}C_6H_5CH_2OP^iPr_2\}]$ (**10a**), $[RuCl_2\{\eta^6{:}\kappa^1(P)\text{-}C_6H_5CH_2CH_2OP^iPr_2\}]$ (**10b**) and $[RuCl_2\{\eta^6{:}\kappa^1(P)\text{-}C_6H_5CH_2CH_2CH_2OP^iPr_2\}]$ (**10c**). Views of the molecular structures, along with selected bonding distances and angles, are shown in Fig. 4–6. All the complexes exhibit the expected pseudo-octahedral three-legged piano-stool geometry with the ruthenium atoms bound to two chlor-

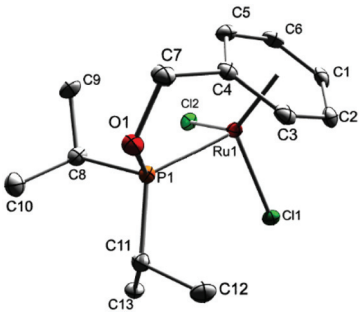

Fig. 4 ORTEP-type view of the structure of complex **10a** showing the crystallographic labelling scheme. Hydrogen atoms have been omitted for clarity. Thermal ellipsoids are drawn at the 30% probability level. Selected bond distances (Å) and angles (°): Ru–C* = 1.694(1); Ru–Cl(1) = 2.420(1); Ru–Cl(2) = 2.414(1); Ru–P(1) = 2.303(1); P(1)–O(1) = 1.641(3); P(1)–C(8) = 1.847(4); P(1)–C(11) = 1.828(4); O(1)–C(7) = 1.445(5); C*–Ru–P(1) = 120.22(3); C*–Ru–Cl(1) = 125.30(3); C*–Ru–Cl(2) = 128.19(3); Cl(1)–Ru–Cl(2) = 85.77(4); Cl(1)–Ru–P(1) = 95.56(4); Cl(2)–Ru–P(1) = 91.87(4); Ru–P(1)–O(1) = 106.0(1); Ru–P(1)–C(8) = 117.7(1); Ru–P(1)–C(11) = 122.2(1); C(8)–P(1)–C(11) = 104.5(2); C(8)–P(1)–O(1) = 104.2(2); C(11)–P(1)–O(1) = 99.3(2); P(1)–O(1)–C(7) = 107.2(3); C* denotes the centroid of the η^6-coordinated arene unit (C(1), C(2), C(3), C(4), C(5) and C(6)).

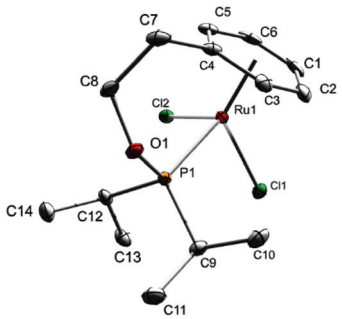

Fig. 5 ORTEP-type view of the structure of complex **10b** showing the crystallographic labelling scheme. Hydrogen atoms have been omitted for clarity. Thermal ellipsoids are drawn at the 30% probability level. Selected bond distances (Å) and angles (°): Ru–C* = 1.713(1); Ru–Cl(1) = 2.414(1); Ru–Cl(2) = 2.421(1); Ru–P(1) = 2.306(1); P(1)–O(1) = 1.630(2); P(1)–C(9) = 1.843(3); P(1)–C(12) = 1.834(3); O(1)–C(8) = 1.443(3); C*–Ru–P(1) = 126.29(2); C*–Ru–Cl(1) = 123.99(2); C*–Ru–Cl(2) = 127.51(2); Cl(1)–Ru–Cl(2) = 87.17(2); Cl(1)–Ru–P(1) = 92.43(2); Cl(2)–Ru–P(1) = 87.55(2); Ru–P(1)–O(1) = 111.04(7); Ru–P(1)–C(9) = 114.76(9); Ru–P(1)–C(12) = 116.73(9); C(9)–P(1)–C(12) = 107.9(1); C(9)–P(1)–O(1) = 104.8(1); C(12)–P(1)–O(1) = 99.9(1); P(1)–O(1)–C(8) = 116.3(1); C* denotes the centroid of the η^6-coordinated arene unit (C(1), C(2), C(3), C(4), C(5) and C(6)).

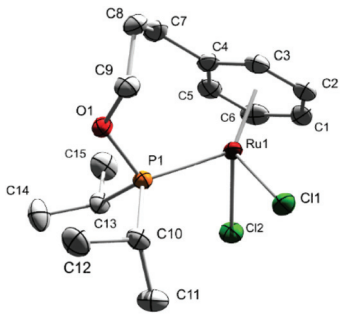

Fig. 6 ORTEP-type view of the structure of complex **10c** showing the crystallographic labelling scheme. Hydrogen atoms have been omitted for clarity. Thermal ellipsoids are drawn at the 30% probability level. Selected bond distances (Å) and angles (°): Ru–C* = 1.723(1); Ru–Cl(1) = 2.417(1); Ru–Cl(2) = 2.417(1); Ru–P(1) = 2.356(1); P(1)–O(1) = 1.621(2); P(1)–C(10) = 1.847(3); P(1)–C(13) = 1.838(3); O(1)–C(9) = 1.448(4); C*–Ru–P(1) = 131.96(2); C*–Ru–Cl(1) = 122.09(2); C*–Ru–Cl(2) = 126.64(2); Cl(1)–Ru–Cl(2) = 87.36(3); Cl(1)–Ru–P(1) = 90.47(3); Cl(2)–Ru–P(1) = 84.89(3); Ru–P(1)–O(1) = 112.99(8); Ru–P(1)–C(10) = 115.1(1); Ru–P(1)–C(13) = 116.4(1); C(10)–P(1)–C(13) = 106.8(1); C(10)–P(1)–O(1) = 103.0(1); C(13)–P(1)–O(1) = 100.3(1); P(1)–O(1)–C(9) = 116.9(1); C* denotes the centroid of the η^6-coordinated arene unit (C(1), C(2), C(3), C(4), C(5) and C(6)).

ide anions, and to the phosphorus atom and tethered phenyl ring of the respective phosphinite ligand. The Ru–Cl, Ru–P and Ru–C* distances are almost identical (±0.05 Å) in the three structures, and very similar to those found for the non-tethered complex $[RuCl_2(\eta^6\text{-}p\text{-cymene})\{^iPr_2POCH_2CH_2CH_2Ph\}]$ (**6c**) discussed above (see Fig. 3). Concerning the interligand angles Cl(1)–Ru–Cl(2), Cl(1)–Ru–P(1) and Cl(2)–Ru–P(1), and those between the centroid of the η^6-coordinated phenyl ring C* and the legs, the most noticeable difference was the increase in

11.7° of the C*–Ru–P(1) angle when passing from [$RuCl_2\{\eta^6{:}\kappa^1(P)\text{-}C_6H_5CH_2OP^iPr_2\}$] (**10a**) to [$RuCl_2\{\eta^6{:}\kappa^1(P)\text{-}C_6H_5CH_2CH_2CH_2OP^iPr_2\}$] (**10c**). Interestingly, a detailed inspection of the Ru–C bond distances indicated that the η^6-coordinated phenyl ring is, in all the complexes, slightly inclined (not completely perpendicular to the Ru–C* axis), with the free end of the ring being further away from the ruthenium atom. This inclination decreases with increasing the spacer's length (*e.g.* Ru–C(1) bond distances of 2.284(2), 2.264(3) and 2.242(3) Å for **10a**, **10b** and **10c**, respectively). In addition, contrary to the case of **10b** and **10c**, the C(7) carbon in **10a** was found to deviate significantly from the mean C(1)-to-C(6) plane (−0.222(5) Å). Taken together, these observations indicate a higher strain of the chelate ring in **10a** *vs.* **10b,c**.

On the other hand, very similar P(1)–O(1) bond lengths were observed in the three structures, with values (1.621(2)–1.641(3) Å) comparable to those previously found in the structures of the tethered complexes **A** and **B** (1.633(2) and 1.625(2) Å, respectively; see Fig. 2) or in that of the non-tethered derivative [$RuCl_2(\eta^6\text{-p-cymene})\{^iPr_2POCH_2CH_2CH_2Ph\}$] (**6c**) (1.619(2) Å). On the contrary, the Ru–P–O and P–O–C angles were affected by the spacer's length, increasing from 106.0(1)° and 99.3(8)° to 112.99(8)° and 116.9(1)°, respectively, when passing from [$RuCl_2\{\eta^6{:}\kappa^1(P)\text{-}C_6H_5CH_2OP^iPr_2\}$] (**10a**) to [$RuCl_2\{\eta^6{:}\kappa^1(P)\text{-}C_6H_5CH_2CH_2CH_2OP^iPr_2\}$] (**10c**).

Finally, the catalytic potential of the tethered complexes [$RuCl_2\{\eta^6{:}\kappa^1(P)\text{-}C_6H_5(CH_2)_nOPR_2\}$] (**9-10a-c**) was investigated. As the catalytic reaction we choose the cross dehydrogenative coupling of hydrosilanes and alcohols (Scheme 5), a process of high interest since it represents an attractive method for the preparation of useful alkoxysilane reagents.[21,30] Also of note is the fact that this process is gaining relevance in the field of hydrogen storage and production.[31] Several studies have shown the utility of ruthenium-based catalysts in this type of transformations,[32] including the arene-ruthenium(II) complexes [{RuCl(μ-Cl)(η^6-*p*-cymene)}$_2$] (**3**)[32b,c,f] and [$RuCl_2(\eta^6$-*p*-cymene)(NHC)] (**11**; NHC = 1-methyl-3-(pyren-1-ylmethyl)-imidazol-2-ylidene).[32g] However, we would like to remark here that there are no previous precedents about the use of tethered-type derivatives.

Initial experiments were performed using dimethylphenylsilane and methanol as model substrates, employing the latter also as the solvent. Thus, in a typical experiment, the corresponding ruthenium complex **9-10a-c** (0.1 mol%) was added under inert atmosphere to a 5 M solution of Me_2PhSiH in MeOH at room temperature, monitoring the course of the reaction by gas chromatography (GC) at 5 minutes intervals. The results obtained are collected in Table 2.

To our delight, all the complexes showed a remarkable activity leading to the complete conversion of the starting silane after only 5–10 min (entries 1–6). The selectivity of the process was also very high in all the cases, the desired methoxydimethyl(phenyl)silane being formed in ≥98% GC yield. Only trace amounts of a byproduct, *i.e.* the disiloxane $Me_2PhSiOSiPhMe_2$, were detected by GC.[33] In a second set of experiments, performed with ruthenium loadings of 0.01 mol%, differences in activity were observed between the complexes (entries 7–12), thus allowing to establish some structure–activity relationships. In particular, the following trends were observed: (i) the activity increases with the length of the spacer within the two series of complexes and (ii) the catalytic performances shown by the diisopropylphosphinite derivatives **10a–c** were higher than those of their corresponding diphenylphosphinite counterparts **9a–c** (entries 10 *vs.* 7, 11 *vs.* 8 and 12 *vs.* 9).[34,35] In particular, the best results were obtained with [$RuCl_2\{\eta^6{:}\kappa^1(P)\text{-}C_6H_5(CH_2)_3OP^iPr_2\}$] (**10c**), which was able to generate the alkoxysilane $Me_2PhSiOMe$ in 98% GC-yield after only 5 min (entry 12), thereby leading to TOF and TON values of 117 600 h^{-1} and 9800, respectively. Reduction of the catalyst loading to 0.005 mol% still produced $Me_2PhSiOMe$ in 98% yield after 1 h (entry 13; TON of 19 600; a kinetic profile of this reaction is given in the ESI file†), but further decrease to 0.001 mol% led to an incomplete transformation with a maximum 57% yield after 48 h (entry 14; TON of 57 000). Remarkably, the effectiveness shown by complex [$RuCl_2\{\eta^6{:}\kappa^1(P)\text{-}C_6H_5(CH_2)_3OP^iPr_2\}$] (**10c**) in this reaction compares favorably with that reported for [{RuCl(μ-Cl)(η^6-*p*-cymene)}$_2$] (**3**) (91% yield of $Me_2PhSiOMe$ after 5 min employing a ruthenium loading of 1 mol%; TOF = 1092 h^{-1})[32c] and [$RuCl_2(\eta^6$-*p*-cymene)(NHC)] (**11**) (>99% yield of

Table 2 Dehydrogenative coupling of dimethylphenylsilane with methanol catalyzed by complexes [$RuCl_2\{\eta^6{:}\kappa^1(P)\text{-}C_6H_5(CH_2)_nOPR_2\}$] (**9-10a-c**)[a]

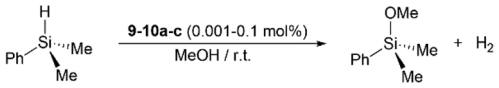

Entry	Catalyst	mol% Ru	Time (min)	Conv.[b] (%)	Yield[b] (%)
1	**9a**	0.1	10	>99	99
2	**9b**	0.1	5	>99	99
3	**9c**	0.1	5	>99	99
4	**10a**	0.1	5	>99	99
5	**10b**	0.1	5	>99	99
6	**10c**	0.1	5	>99	98 (85)[c]
7	**9a**	0.01	120	>99	99
8	**9b**	0.01	100	>99	98
9	**9c**	0.01	50	>99	98
10	**10a**	0.01	70	>99	98
11	**10b**	0.01	40	>99	98
12	**10c**	0.01	5	>99	98
13	**10c**	0.005	60	>99	98
14	**10c**	0.001	2880	60	57

[a] Reactions were performed under argon atmosphere employing 5 mmol of Me_2PhSiH and 1 mL of MeOH. [b] Determined by GC. Differences between conversions and yields correspond to the disiloxane $Me_2PhSiOSiPhMe_2$. [c] Isolated yield after work-up (see the Experimental section).

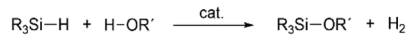

Scheme 5 The catalytic cross dehydrogenative coupling of silanes and alcohols.

$Me_2PhSiOMe$ after 10 min employing a ruthenium loading of 0.1 mol%; TOF = 6000 h^{-1}).[32g]

The scope of $[RuCl_2\{\eta^6{:}\kappa^1(P)\text{-}C_6H_5(CH_2)_3OP^iPr_2\}]$ (**10c**) was next explored varying the nature of the alcohol (Scheme 6). For convenience, we decided to use a catalyst loading of 0.1 mol% in all the experiments. The results obtained showed that the efficiency of this ruthenium catalyst is markedly influenced by the steric constrains associated to the substrates. Thus, although the reactions of dimethylphenylsilane with other primary alcohols also generated the corresponding alkoxysilanes in high yield (>92% by GC, with isolated yields ≥84%), longer reaction times were systematically required.

The cross dehydrogenative coupling of Me_2PhSiH with 2-propanol was also satisfactorily achieved after 2 h employing 0.1 mol% of **10c**, but when bulkier secondary alcohols (2-butanol or cycloheptanol) were employed, an increase in the catalyst loading to 1 mol% was required to generate the corresponding alkoxysilanes in high yield (employing 0.1 mol% of **10c** incomplete reactions were observed even after 24 h). An increase of the ruthenium loading to 1 mol% was also needed in the reaction of Me_2PhSiH with propargyl alcohol, for which a surprisingly clean transformation occurred without any side-reaction associated with the activation of the terminal C≡C bond.[36] The effect of sterics on the activity of complex

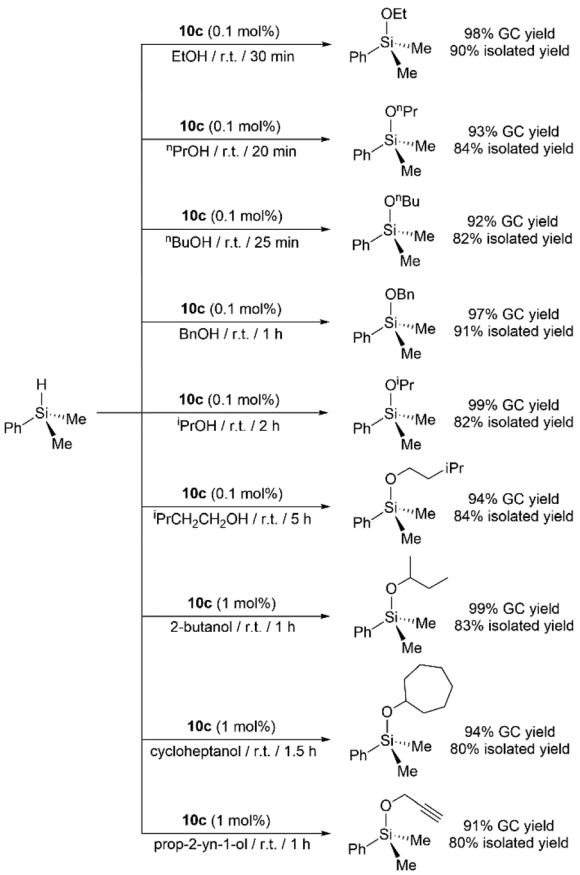

Scheme 6 Dehydrogenative coupling of Me_2PhSiH with different alcohols catalyzed by **10c**.

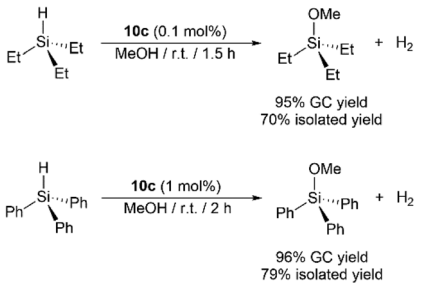

Scheme 7 Dehydrogenative coupling of Et_3SiH and Ph_3SiH with methanol catalyzed by **10c**.

10c was also evidenced in the dehydrogenative coupling reactions of triethylsilane and triphenylsilane with methanol (Scheme 7), requiring, when compared to Me_2PhSiH, a longer reaction time in the first case, and an increase of the catalyst loading in the second, to obtain the desired alkoxysilanes in high yields.

Conclusions

In summary, we have synthesized and structurally characterized a series of half-sandwich ruthenium(II) complexes featuring tethered arene-phosphinite ligands, species underrepresented to date in the literature. The synthesis of compounds $[RuCl_2\{\eta^6{:}\kappa^1(P)\text{-}C_6H_5(CH_2)_nOPR_2\}]$ (**9-10a-c**) was easily accomplished in two steps from the readily accessible phosphinite ligands $R_2PO(CH_2)_nPh$ and dimers $[\{RuCl(\mu\text{-}Cl)(\eta^6\text{-arene})\}_2]$ (arene = *p*-cymene, benzene). Given the greater lability of the benzene *vs.* *p*-cymene ligand, the use of dimer $[\{RuCl(\mu\text{-}Cl)(\eta^6\text{-benzene})\}_2]$ resulted in general more convenient, allowing faster arene exchange processes. The catalytic utility of complexes $[RuCl_2\{\eta^6{:}\kappa^1(P)\text{-}C_6H_5(CH_2)_nOPR_2\}]$ (**9-10a-c**) was also demonstrated, finding that they are able to promote efficiently and under mild conditions the cross dehydrogenative coupling of hydrosilanes and alcohols. To the best of our knowledge, the involvement of tethered species in this catalytic transformation is unprecedented. Interestingly, the most active complex found in this study, namely $[RuCl_2\{\eta^6{:}\kappa^1(P)\text{-}C_6H_5(CH_2)_3OP^iPr_2\}]$ (**10c**), was more effective than other (η^6-arene)-ruthenium(II)-type catalysts previously described.

Experimental

General methods

Synthetic procedures were performed under an atmosphere of dry argon using vacuum-line and standard Schlenk or sealed-tube techniques. Organic solvents were dried by standard methods and distilled under argon before use.[37] All reagents were obtained from commercial suppliers and used without further purification with the exception of the phosphinite ligands $R_2PO(CH_2)_nPh$ (**1-2a-c**),[22] and the ruthenium(II) complexes $[\{RuCl(\mu\text{-}Cl)(\eta^6\text{-arene})\}_2]$ (arene = *p*-cymene (**3**), benzene (**4**)) and

$[RuCl_2(\eta^6\text{-}p\text{-cymene})(PPh_3)]$,[24] which were prepared by following the methods reported in the literature. NMR spectra were recorded at 25 °C on Bruker DPX-300 or AV400 instruments. $^{13}C\{^1H\}$ and ^1H NMR chemical shifts were referenced to the residual signal of deuterated solvent. All data are reported in ppm downfield from $(CH_3)_4Si$. $^{31}P\{^1H\}$ NMR chemical shifts were referenced to 85% H_3PO_4 as external standard. DEPT experiments have been carried out for all the compounds reported in this paper. GC measurements were made on a Hewlett Packard HP6890 apparatus (Supelco Beta-Dex™ 120 column, 30 m length, 250 μm diameter). Elemental analyses were provided by the Analytical Service of the Instituto de Investigaciones Químicas (IIQ-CSIC) of Seville. For column chromatography, Merck silica gel 60 (230–400 mesh) was employed.

General procedure for the preparation of complexes $[RuCl_2(\eta^6\text{-}p\text{-cymene})\{R_2PO(CH_2)_nPh\}]$ (R = Ph, *n* = 1 (5a), 2 (5b), 3 (5c); R = ^{i}Pr, *n* = 1 (6a), 2 (6b), 3 (6c)) and $[RuCl_2(\eta^6\text{-benzene})\{R_2PO(CH_2)_nPh\}]$ (R = Ph, *n* = 1 (7a), 2 (7b), 3 (7c); R = ^{i}Pr, *n* = 1 (8a), 2 (8b), 3 (8c))

A suspension of the corresponding dimer $[\{RuCl(\mu\text{-}Cl)(\eta^6\text{-arene})\}_2]$ (arene = *p*-cymene (**3**), benzene (**4**); 0.3 mmol) and phosphinite ligand $R_2PO(CH_2)_nPh$ (**1-2a-c**; 0.8 mmol) in tetrahydrofuran (20 mL) was stirred for 1 (starting from **3**) or 12 h (starting from **4**) at room temperature. The resulting solution was then evaporated to dryness, the oily residue formed dissolved in the minimum amount of CH_2Cl_2 (*ca.* 5 mL), and the product precipitated by adding 20 mL of a diethyl ether/hexane mixture (1 : 1 v/v). The same precipitation procedure was repeated twice more and the reddish orange solid was finally washed with diethyl ether (5 mL) and dried *in vacuo*. Characterization data for the resulting complexes **5-8a-c** are as follows: (**5a**): Yield: 0.298 g (83%). $^{31}P\{^1H\}$ NMR ($CDCl_3$): δ = 111.6 (s) ppm. ^1H NMR ($CDCl_3$): δ = 8.03–7.96 (m, 4H, Ph), 7.43–7.32 (m, 11H, Ph), 5.25 and 5.20 (d, 2H each, $^3J_{HH}$ = 5.9 Hz, CH of *p*-cymene), 4.86 (d, 2H, $^3J_{PH}$ = 5.1 Hz, OCH_2), 2.69 (sept, 1H, $^3J_{HH}$ = 6.9 Hz, C*H*Me_2), 1.83 (s, 3H, Me), 1.08 (d, 6H, $^3J_{HH}$ = 6.9 Hz, CH*Me*$_2$) ppm. $^{13}C\{^1H\}$ NMR ($CDCl_3$): δ = 137.8 (d, $^3J_{PC}$ = 8.5 Hz, C_{ipso} of Ph), 136.3 (d, $^1J_{PC}$ = 48.4 Hz, C_{ipso} of PPh), 132.5 (d, J_{PC} = 11.1 Hz, CH_{ortho} or CH_{meta} of PPh), 130.9 (s, CH_{para} of PPh), 128.5 and 127.0 (s, CH_{ortho} and CH_{meta} of Ph), 127.9 (d, J_{PC} = 10.2 Hz, CH_{ortho} or CH_{meta} of PPh), 127.8 (s, CH_{para} of Ph), 111.9 and 97.6 (s, C of *p*-cymene), 90.6 (d, $^2J_{PC}$ = 3.4 Hz, CH of *p*-cymene), 87.5 (d, $^2J_{PC}$ = 5.5 Hz, CH of *p*-cymene), 68.5 (s, OCH_2), 30.1 (s, *C*HMe_2), 21.8 (s, CH*Me*$_2$), 17.5 (s, Me) ppm. Elemental analysis calcd (%) for $C_{29}H_{31}Cl_2OPRu$: C 58.20, H 5.22; found: C 57.93, H 5.33. (**5b**): Yield: 0.272 g (74%). $^{31}P\{^1H\}$ NMR (CD_2Cl_2): δ = 110.1 (s) ppm. ^1H NMR (CD_2Cl_2): δ = 7.87–7.81 (m, 4H, Ph), 7.43–7.28 (m, 11H, Ph), 5.16 and 5.04 (d, 2H each, $^3J_{HH}$ = 6.0 Hz, CH of *p*-cymene), 3.95 (td, 2H, $^3J_{HH}$ = 6.0 Hz, $^3J_{PH}$ = 5.1 Hz, OCH_2), 2.96 (t, 2H, $^3J_{HH}$ = 6.0 Hz, CH_2Ph), 2.53 (sept, 1H, $^3J_{HH}$ = 6.9 Hz, C*H*Me_2), 1.74 (s, 3H, Me), 1.08 (d, 6H, $^3J_{HH}$ = 6.9 Hz, CH*Me*$_2$) ppm. $^{13}C\{^1H\}$ NMR (CD_2Cl_2): δ = 138.7 (s, C_{ipso} of Ph), 136.5 (d, $^1J_{PC}$ = 48.0 Hz, C_{ipso} of PPh), 132.4 (d, J_{PC} = 10.8 Hz, CH_{ortho} or CH_{meta} of PPh), 130.7 (s, CH_{para} of PPh), 129.3 and 128.5 (s, CH_{ortho} and CH_{meta} of Ph), 127.7 (d, J_{PC} = 10.1 Hz, CH_{ortho} or CH_{meta} of PPh), 126.6 (s, CH_{para} of Ph), 110.9 and 98.0 (s, C of *p*-cymene), 90.1 (d, $^2J_{PC}$ = 3.5 Hz, CH of *p*-cymene), 87.7 (d, $^2J_{PC}$ = 5.4 Hz, CH of *p*-cymene), 68.0 (d, $^2J_{PC}$ = 4.0 Hz, OCH_2), 37.1 (d, $^3J_{PC}$ = 7.6 Hz, *C*H_2Ph), 30.2 (s, *C*HMe_2), 21.6 (s, CH*Me*$_2$), 17.2 (s, Me) ppm. Elemental analysis calcd (%) for $C_{30}H_{33}Cl_2OPRu$: C 58.83, H 5.43; found: C 58.75, H 5.37. (**5c**): Yield: 0.327 g (87%). $^{31}P\{^1H\}$ NMR (CD_2Cl_2): δ = 109.5 (s) ppm. ^1H NMR (CD_2Cl_2): δ = 7.95–7.89 (m, 4H, Ph), 7.43–7.20 (m, 11H, Ph), 5.24 and 5.17 (d, 2H each, $^3J_{HH}$ = 5.7 Hz, CH of *p*-cymene), 3.82–3.77 (m, 2H, OCH_2), 2.76 (t, 2H, $^3J_{HH}$ = 7.5 Hz, CH_2Ph), 2.61 (sept, 1H, $^3J_{HH}$ = 6.9 Hz, C*H*Me_2), 2.03–1.96 (m, 2H, CH_2), 1.81 (s, 3H, Me), 1.10 (d, 6H, $^3J_{HH}$ = 6.9 Hz, CH*Me*$_2$) ppm. $^{13}C\{^1H\}$ NMR (CD_2Cl_2): δ = 141.5 (s, C_{ipso} of Ph), 136.6 (d, $^1J_{PC}$ = 48.1 Hz, C_{ipso} of PPh), 132.5 (d, J_{PC} = 10.8 Hz, CH_{ortho} or CH_{meta} of PPh), 130.7 (s, CH_{para} of PPh), 128.4 (s, CH_{ortho} and CH_{meta} of Ph), 127.7 (d, J_{PC} = 10.0 Hz, CH_{ortho} or CH_{meta} of PPh), 125.9 (s, CH_{para} of Ph), 110.9 and 97.5 (s, C of *p*-cymene), 90.6 (d, $^2J_{PC}$ = 3.6 Hz, CH of *p*-cymene), 87.6 (d, $^2J_{PC}$ = 5.4 Hz, CH of *p*-cymene), 66.7 (d, $^2J_{PC}$ = 3.9 Hz, OCH_2), 32.2 (d, $^3J_{PC}$ = 7.1 Hz, CH_2), 32.1 (s, *C*H_2Ph), 30.2 (s, *C*HMe_2), 21.6 (s, CH*Me*$_2$), 17.3 (s, Me) ppm. Elemental analysis calcd (%) for $C_{31}H_{35}Cl_2OPRu$: C 59.43, H 5.63; found: C 59.24, H 5.64. (**6a**): Yield: 0.255 g (80%). $^{31}P\{^1H\}$ NMR ($CDCl_3$): δ = 151.9 (s) ppm. ^1H NMR ($CDCl_3$): δ = 7.42 (br s, 5H, Ph), 5.47 and 5.40 (d, 2H each, $^3J_{HH}$ = 5.9 Hz, CH of *p*-cymene), 5.00 (d, 2H, $^3J_{PH}$ = 3.6 Hz, OCH_2), 2.98–2.87 (m, 3H, C*H*Me_2 and PC*H*Me_2), 2.10 (s, Me), 1.48–1.30 (m, 18H, CH*Me*$_2$ and PCH*Me*$_2$) ppm. $^{13}C\{^1H\}$ NMR ($CDCl_3$): δ = 137.7 (d, $^3J_{PC}$ = 6.4 Hz, C_{ipso} of Ph), 128.7 and 127.1 (s, CH_{ortho} and CH_{meta} of Ph), 128.1 (s, CH_{para} of Ph), 108.4 and 97.5 (s, C of *p*-cymene), 88.5 (d, $^2J_{PC}$ = 3.2 Hz, CH of *p*-cymene), 87.7 (d, $^2J_{PC}$ = 4.2 Hz, CH of *p*-cymene), 69.2 (d, $^2J_{PC}$ = 9.2 Hz, OCH_2), 30.5 (s, *C*HMe_2), 30.2 (d, $^1J_{PC}$ = 20.5 Hz, P*C*HMe_2), 22.1 (s, CH*Me*$_2$), 18.1 and 17.8 (s, PCH*Me*$_2$), 18.0 (s, Me) ppm. Elemental analysis calcd (%) for $C_{23}H_{35}Cl_2OPRu$: C 52.08, H 6.65; found: C 52.15, H 6.71. (**6b**): Yield: 0.251 g (77%). $^{31}P\{^1H\}$ NMR ($CDCl_3$): δ = 150.7 (s) ppm. ^1H NMR ($CDCl_3$): δ = 7.39–7.25 (m, 5H, Ph), 5.32 and 5.27 (d, 2H each, $^3J_{HH}$ = 6.2 Hz, CH of *p*-cymene), 4.23 (td, 2H, $^3J_{HH}$ = 6.3 Hz, $^3J_{PH}$ = 3.9 Hz, OCH_2), 3.04 (t, 2H, $^3J_{HH}$ = 6.3 Hz, CH_2Ph), 2.89–2.77 (m, 3H, C*H*Me_2 and PC*H*Me_2), 2.06 (s, Me), 1.38–1.19 (m, 18H, CH*Me*$_2$ and PCH*Me*$_2$) ppm. $^{13}C\{^1H\}$ NMR ($CDCl_3$): δ = 138.0 (s, C_{ipso} of Ph), 128.9 and 128.6 (s, CH_{ortho} and CH_{meta} of Ph), 126.8 (s, CH_{para} of Ph), 107.5 and 96.8 (s, C of *p*-cymene), 88.8 (d, $^2J_{PC}$ = 3.2 Hz, CH of *p*-cymene), 87.7 (d, $^2J_{PC}$ = 4.1 Hz, CH of *p*-cymene), 68.0 (d, $^2J_{PC}$ = 11.3 Hz, OCH_2), 37.6 (d, $^3J_{PC}$ = 5.6 Hz, *C*H_2Ph), 30.0 (s, *C*HMe_2), 29.4 (d, $^1J_{PC}$ = 19.7 Hz, P*C*HMe_2), 22.1 (s, CH*Me*$_2$), 17.9 (s, Me), 17.4 (s, PCH*Me*$_2$) ppm. Elemental analysis calcd (%) for $C_{24}H_{37}Cl_2OPRu$: C 52.94, H 6.85; found: C 53.05, H 6.91. (**6c**): Yield: 0.235 g (70%). $^{31}P\{^1H\}$ NMR ($CDCl_3$): δ = 150.3 (s) ppm. ^1H NMR ($CDCl_3$): δ = 7.37–7.14 (m, 5H, Ph), 5.50 and 5.41 (d, 2H each, $^3J_{HH}$ = 2.0 Hz, CH of *p*-cymene), 4.01–3.95 (m, 2H, OCH_2), 2.95–2.77 (m, 5H, CH_2Ph, C*H*Me_2 and PC*H*Me_2), 2.13 (s, Me), 2.10–2.04 (m, 2H, CH_2), 1.31–1.24 (m, 18H, CH*Me*$_2$ and PCH*Me*$_2$) ppm. ^{13}C

{^{1}H} NMR ($CDCl_3$): δ = 141.1 (s, C_{ipso} of Ph), 128.6 and 128.4 (s, CH_{ortho} and CH_{meta} of Ph), 126.2 (s, CH_{para} of Ph), 108.2 and 97.0 (s, C of *p*-cymene), 88.6 (s, CH of *p*-cymene), 87.7 (d, $^2J_{PC}$ = 4.5 Hz, CH of *p*-cymene), 67.2 (d, $^2J_{PC}$ = 10.3 Hz, OCH_2), 32.8 (d, $^3J_{PC}$ = 5.8 Hz, CH_2), 32.2 (s, *C*H_2Ph), 30.1 (s, *C*HMe$_2$), 29.9 (d, $^1J_{PC}$ = 20.4 Hz, P*C*HMe$_2$), 22.1 (s, CH*Me*$_2$), 18.0 and 17.6 (s, PCH*Me*$_2$), 17.9 (s, Me) ppm. Elemental analysis calcd (%) for $C_{25}H_{39}Cl_2OPRu$: C 53.76, H 7.04; found: C 53.71, H 7.11. (**7a**): Yield: 0.277 g (85%). $^{31}P\{^1H\}$ NMR ($CDCl_3$): δ = 111.2 (s) ppm. ^{1}H NMR ($CDCl_3$): δ = 8.04–7.97 (m, 4H, Ph), 7.47–7.35 (m, 11H, Ph), 5.42 (d, 6H, $^3J_{HH}$ = 1.0 Hz, C_6H_6), 4.96 (d, 2H, $^3J_{PH}$ = 5.7 Hz, OCH_2) ppm. $^{13}C\{^1H\}$ NMR ($CDCl_3$): δ = 137.6 (d, $^3J_{PC}$ = 8.1 Hz, C_{ipso} of Ph), 136.4 (d, $^1J_{PC}$ = 51.6 Hz, C_{ipso} of PPh), 132.3 (d, J_{PC} = 11.2 Hz, CH_{ortho} or CH_{meta} of PPh), 131.2 (s, CH_{para} of PPh), 128.6 and 127.4 (s, CH_{ortho} and CH_{meta} of Ph), 128.2 (d, J_{PC} = 10.4 Hz, CH_{ortho} or CH_{meta} of PPh), 128.0 (s, CH_{para} of Ph), 90.1 (d, $^2J_{PC}$ = 3.2 Hz, C_6H_6), 69.0 (s, OCH_2) ppm. Elemental analysis calcd (%) for $C_{25}H_{23}Cl_2OPRu$: C 55.36, H 4.27; found: C 55.29, H 4.39. (**7b**): Yield: 0.300 g (90%). $^{31}P\{^1H\}$ NMR ($CDCl_3$): δ = 109.0 (s) ppm. ^{1}H NMR ($CDCl_3$): δ = 7.92–7.86 (m, 4H, Ph), 7.43–7.28 (m, 11H, Ph), 5.21 (s, 6H, C_6H_6), 4.07 (td, 2H, $^3J_{HH}$ = 6.0 Hz, $^3J_{PH}$ = 4.5 Hz, OCH_2), 2.97 (t, 2H, $^3J_{HH}$ = 6.0 Hz, C*H*$_2$Ph) ppm. $^{13}C\{^1H\}$ NMR ($CDCl_3$): δ = 139.0 (s, C_{ipso} of Ph), 136.3 (d, $^1J_{PC}$ = 51.2 Hz, C_{ipso} of PPh), 132.2 (d, J_{PC} = 11.0 Hz, CH_{ortho} or CH_{meta} of PPh), 131.1 (s, CH_{para} of PPh), 129.3 and 128.6 (s, CH_{ortho} and CH_{meta} of Ph), 128.0 (d, J_{PC} = 10.2 Hz, CH_{ortho} or CH_{meta} of PPh), 126.7 (s, CH_{para} of Ph), 90.0 (s, C_6H_6), 68.4 (s, OCH_2), 37.2 (d, $^3J_{PC}$ = 10.0 Hz, *C*H_2Ph) ppm. Elemental analysis calcd (%) for $C_{26}H_{25}Cl_2OPRu$: C 56.12, H 4.53; found: C 56.03, H 4.48. (**7c**): Yield: 0.287 g (84%). $^{31}P\{^1H\}$ NMR ($CDCl_3$): δ = 109.3 (s) ppm. ^{1}H NMR ($CDCl_3$): δ = 7.97–7.92 (m, 4H, Ph), 7.45–7.18 (m, 11H, Ph), 5.39 (s, 6H, C_6H_6), 3.95–3.89 (m, 2H, OCH_2), 2.76 (t, 2H, $^3J_{HH}$ = 7.5 Hz, C*H*$_2$Ph), 2.01–1.96 (m, 2H, CH_2) ppm. $^{13}C\{^1H\}$ NMR ($CDCl_3$): δ = 141.3 (s, C_{ipso} of Ph), 136.6 (d, $^1J_{PC}$ = 51.5 Hz, C_{ipso} of PPh), 132.2 (d, J_{PC} = 10.7 Hz, CH_{ortho} or CH_{meta} of PPh), 131.1 (s, CH_{para} of PPh), 128.5 (s, CH_{ortho} and CH_{meta} of Ph), 128.1 (d, J_{PC} = 10.0 Hz, CH_{ortho} or CH_{meta} of PPh), 126.0 (s, CH_{para} of Ph), 90.0 (s, C_6H_6), 67.2 (s, OCH_2), 32.2 (s, CH_2 and *C*H_2Ph) ppm. Elemental analysis calcd (%) for $C_{27}H_{27}Cl_2OPRu$: C 56.85, H 4.77; found: C 56.78, H 4.69. (**8a**): Yield: 0.188 g (66%). $^{31}P\{^1H\}$ NMR ($CDCl_3$): δ = 150.9 (s) ppm. ^{1}H NMR ($CDCl_3$): δ = 7.40 (br s, 5H, Ph), 5.66 (s, 6H, C_6H_6), 5.02 (d, 2H, $^3J_{PH}$ = 4.8 Hz, OCH_2), 3.11–3.00 (m, 2H, P*C*HMe$_2$), 1.46–1.30 (m, 12H, PCH*Me*$_2$) ppm. $^{13}C\{^1H\}$ NMR ($CDCl_3$): δ = 138.0 (s, C_{ipso} of Ph), 128.7 and 126.4 (s, CH_{ortho} and CH_{meta} of Ph), 127.9 (s, CH_{para} of Ph), 88.6 (d, $^2J_{PC}$ = 2.4 Hz, C_6H_6), 68.9 (s, OCH_2), 31.2 (d, $^1J_{PC}$ = 23.5 Hz, P*C*HMe$_2$), 18.4 (s, PCH*Me*$_2$) ppm. Elemental analysis calcd (%) for $C_{19}H_{27}Cl_2OPRu$: C 48.11, H 5.74; found: C 48.24, H 5.80. (**8b**): Yield: 0.208 g (71%). $^{31}P\{^1H\}$ NMR ($CDCl_3$): δ = 148.5 (s) ppm. ^{1}H NMR ($CDCl_3$): δ = 7.39–7.33 (m, 5H, Ph), 5.48 (s, 6H, C_6H_6), 4.09 (td, 2H, $^3J_{HH}$ = 6.0 Hz, $^3J_{PH}$ = 3.3 Hz, OCH_2), 2.97 (t, 2H, $^3J_{HH}$ = 6.0 Hz, C*H*$_2$Ph), 2.95–2.86 (m, 2H, P*C*HMe$_2$), 1.35–1.21 (m, 12H, PCH*Me*$_2$) ppm. $^{13}C\{^1H\}$ NMR ($CDCl_3$): δ = 138.7 (s, C_{ipso} of Ph), 129.2 and 128.5 (s, CH_{ortho} and CH_{meta} of Ph), 126.7 (s, CH_{para} of Ph), 88.4 (d, $^2J_{PC}$ = 3.0 Hz, C_6H_6), 68.6 (d, $^2J_{PC}$ = 7.1 Hz, OCH_2), 37.4 (d, $^2J_{PC}$ = 7.1 Hz, *C*H_2Ph), 30.7 (d, $^1J_{PC}$ = 23.2 Hz, P*C*HMe$_2$), 18.2 and 18.0 (s, PCH*Me*$_2$) ppm. Elemental analysis calcd (%) for $C_{20}H_{29}Cl_2OPRu$: C 49.11, H 5.99; found: C 49.22, H 6.01. (**8c**): Yield: 0.214 g (71%). $^{31}P\{^1H\}$ NMR ($CDCl_3$): δ = 148.0 (s) ppm. ^{1}H NMR ($CDCl_3$): δ = 7.38–7.22 (m, 5H, Ph), 5.61 (s, 6H, C_6H_6), 3.92–3.86 (m, 2H, OCH_2), 2.98–2.90 (m, 2H, P*C*HMe$_2$), 2.77 (t, 2H, $^3J_{HH}$ = 7.5 Hz, C*H*$_2$Ph), 2.05–1.98 (m, 2H, CH_2), 1.40–1.25 (m, 12H, PCH*Me*$_2$) ppm. $^{13}C\{^1H\}$ NMR ($CDCl_3$): δ = 141.2 (s, C_{ipso} of Ph), 128.5 and 128.4 (s, CH_{ortho} and CH_{meta} of Ph), 126.1 (s, CH_{para} of Ph), 88.4 (s, C_6H_6), 67.1 (d, $^2J_{PC}$ = 6.6 Hz, OCH_2), 32.3 (d, $^3J_{PC}$ = 6.6 Hz, CH_2), 32.0 (s, *C*H_2Ph), 30.9 (d, $^1J_{PC}$ = 24.0 Hz, P*C*HMe$_2$), 18.2 (s, PCH*Me*$_2$) ppm. Elemental analysis calcd (%) for $C_{21}H_{31}Cl_2OPRu$: C 50.20, H 6.22; found: C 50.11, H 6.24.

Synthesis of complexes [$RuCl_2\{\eta^6$:κ^1(*P*)-$C_6H_5(CH_2)_nOPPh_2\}$] (*n* = 1 (9a), 2 (9b), 3 (9c))

In Teflon-capped sealed tube, 0.1 mmol of the corresponding ruthenium complex [$RuCl_2(\eta^6$-benzene)$\{Ph_2PO(CH_2)_nPh\}$] (**7a–c**) were dissolved in 20 mL of 1,2-dichloroethane and the resulting solution stirred at 120 °C for the indicated time (see below). The mixture was then evaporated to dryness, the oily residue formed dissolved in the minimum amount of CH_2Cl_2 (*ca.* 0.5 mL), and the product precipitated by adding 20 mL of a diethyl ether/hexane mixture (1 : 1 v/v). The same precipitation procedure was repeated twice more and the brown solid was finally washed with diethyl ether (5 mL) and dried *in vacuo*. Characterization data for the resulting complexes **9a–c** are as follows: (**9a**): Reaction time: 2 h. Yield: 0.028 g (61%). $^{31}P\{^1H\}$ NMR ($CDCl_3$): δ = 158.6 (s) ppm. ^{1}H NMR ($CDCl_3$): δ = 7.77–7.46 (m, 10H, PPh), 6.41 (br, 1H, CH_{para} of Ph), 6.10 (br, 2H, CH_{meta} of Ph), 5.39 (br, 2H, CH_{ortho} of Ph), 4.74 (d, 2H, $^3J_{PH}$ = 16.2 Hz, OCH_2) ppm. $^{13}C\{^1H\}$ NMR (CD_2Cl_2): δ = 134.0 (d, $^1J_{PC}$ = 54.0 Hz, C_{ipso} of PPh), 132.2 (s, CH_{para} of PPh), 131.5 (d, J_{PC} = 10.5 Hz, CH_{ortho} or CH_{meta} of PPh), 128.1 (d, J_{PC} = 11.4 Hz, CH_{ortho} or CH_{meta} of PPh), 108.8 (s, C_{ipso} of Ph), 98.1, 94.1 and 80.6 (s, CH of Ph), 67.8 (s, OCH_2) ppm. Elemental analysis calcd (%) for $C_{19}H_{17}Cl_2OPRu$: C 49.15, H 3.69; found: C 49.22, H 3.76. (**9b**): Reaction time: 5 h. Yield: 0.039 g (82%). $^{31}P\{^1H\}$ NMR ($CDCl_3$): δ = 121.5 (s) ppm. ^{1}H NMR ($CDCl_3$): δ = 7.88–7.82 (m, 4H, PPh), 7.41–7.38 (m, 6H, PPh), 6.49 (t, 1H, $^3J_{HH}$ = 6.0 Hz, CH_{para} of Ph), 5.88 (t, 2H, $^3J_{HH}$ = 6.0 Hz, CH_{meta} of Ph), 5.24 (d, 2H, $^3J_{HH}$ = 6.0 Hz, CH_{ortho} of Ph), 4.36 (dt, 2H, $^3J_{PH}$ = 19.8 Hz, $^3J_{HH}$ = 4.8 Hz, OCH_2), 2.63 (t, 2H, $^3J_{HH}$ = 4.8 Hz, C*H*$_2$Ph) ppm. $^{13}C\{^1H\}$ NMR (DMSO-d_6): δ = 136.5 (d, $^1J_{PC}$ = 54.6 Hz, C_{ipso} of PPh), 132.3 (d, J_{PC} = 11.1 Hz, CH_{ortho} or CH_{meta} of PPh), 131.1 (s, CH_{para} of PPh), 128.1 (d, J_{PC} = 10.6 Hz, CH_{ortho} or CH_{meta} of PPh), 102.2 (d, $^2J_{PC}$ = 11.3 Hz, C_{ipso} of Ph), 92.6 (d, $^2J_{PC}$ = 4.6 Hz, CH of Ph), 91.3 and 85.9 (s, CH of Ph), 68.0 (s, OCH_2), 29.5 (s, *C*H_2Ph) ppm. Elemental analysis calcd (%) for $C_{20}H_{19}Cl_2OPRu$: C 50.22, H 4.00; found: C 50.31, H 3.98. (**9c**):[16] Reaction time: 10 h. Yield: 0.039 g (79%). $^{31}P\{^1H\}$ NMR (CD_2Cl_2): δ = 119.3 (s) ppm. ^{1}H NMR (CD_2Cl_2): δ = 7.90–7.85 (m, 4H, PPh), 7.42–7.39 (m, 6H, PPh), 6.28 (t, 1H, $^3J_{HH}$ = 4.5

Hz, CH_{para} of Ph), 5.82 (t, 2H, $^3J_{HH}$ = 4.5 Hz, CH_{meta} of Ph), 5.09 (d, 2H, $^3J_{HH}$ = 4.5 Hz, CH_{ortho} of Ph), 4.90 (dt, 2H, $^3J_{PH}$ = 12.6 Hz, $^3J_{HH}$ = 4.5 Hz, OCH_2), 2.79 (t, 2H, $^3J_{HH}$ = 5.1 Hz, CH_2Ph), 2.24–2.18 (m, 2H, CH_2) ppm. $^{13}C\{^1H\}$ NMR (CD_2Cl_2): δ = 137.7 (d, $^1J_{PC}$ = 54.5 Hz, C_{ipso} of PPh), 131.5 (d, J_{PC} = 10.8 Hz, CH_{ortho} or CH_{meta} of PPh), 130.5 (s, CH_{para} of PPh), 127.7 (d, J_{PC} = 10.7 Hz, CH_{ortho} or CH_{meta} of PPh), 97.9 (d, $^2J_{PC}$ = 10.5 Hz, CH of Ph), 96.0 (s, C_{ipso} of Ph), 93.4 and 84.5 (s, CH of Ph), 66.0 (s, OCH_2), 26.9 and 24.1 (s, CH_2 and CH_2Ph) ppm.

Synthesis of complexes $[RuCl_2\{\eta^6{:}\kappa^1(P)\text{-}C_6H_5(CH_2)_nOP^iPr_2\}]$ (n = 1 (**10a**), 2 (**10b**), 3 (**10c**))

Complexes **10a–c**, isolated as brown solids, were prepared as described for **9a–c** starting from 0.1 mmol of the corresponding ruthenium complex $[RuCl_2(\eta^6\text{-}p\text{-cymene})\{^iPr_2PO(CH_2)_nPh\}]$ (**6a–c**; method A) or $[RuCl_2(\eta^6\text{-benzene})\{^iPr_2PO(CH_2)_nPh\}]$ (**8a–c**; method B). Characterization data are as follows: (**10a**): Reaction time: 1 h (method A) or 0.5 h (method B). Yield: 0.026 g (65%) (method A) or 0.024 g (62%) (method B). $^{31}P\{^1H\}$ NMR ($CDCl_3$): δ = 206.2 (s) ppm. ^1H NMR (CD_2Cl_2): δ = 6.35 (t, 1H, $^3J_{HH}$ = 5.7 Hz, CH_{para} of Ph), 6.01 (t, 2H, $^3J_{HH}$ = 5.7 Hz, CH_{meta} of Ph), 5.23 (d, 2H, $^3J_{HH}$ = 5.7 Hz, CH_{ortho} of Ph), 4.60 (d, 2H, $^3J_{PH}$ = 13.5 Hz, OCH_2), 2.61–2.49 (m, 2H, $PCHMe_2$), 1.16–1.40 (m, 12H, $PCHMe_2$) ppm. $^{13}C\{^1H\}$ NMR ($CDCl_3$): δ = 110.2 (s, C_{ipso} of Ph), 100.0 and 75.6 (s, CH of Ph), 91.7 (d, $^2J_{PC}$ = 13.4 Hz, CH of Ph), 72.2 (s, OCH_2), 30.2 (d, $^1J_{PC}$ = 25.5 Hz, $PCHMe_2$), 16.9 and 16.2 (s, $PCHMe_2$) ppm. Elemental analysis calcd (%) for $C_{13}H_{21}Cl_2OPRu$: C 39.40, H 5.34; found: C 39.22, H 5.30. (**10b**): Reaction time: 1.5 h (method A) or 1 h (method B). Yield: 0.027 g (67%) (method A) or 0.029 g (70%) (method B). $^{31}P\{^1H\}$ NMR ($CDCl_3$): δ = 159.8 (s) ppm. ^1H NMR (CD_2Cl_2): δ = 6.38 (t, 1H, $^3J_{HH}$ = 5.7 Hz, CH_{para} of Ph), 5.80 (t, 2H, $^3J_{HH}$ = 5.7 Hz, CH_{meta} of Ph), 5.16 (d, 2H, $^3J_{HH}$ = 5.7 Hz, CH_{ortho} of Ph), 4.07 (dt, 2H, $^3J_{PH}$ = 16.2 Hz, $^3J_{HH}$ = 4.8 Hz, OCH_2), 3.00–2.89 (m, 2H, $PCHMe_2$), 2.45 (t, 2H, $^3J_{HH}$ = 4.8 Hz, CH_2Ph), 1.19–1.27 (m, 12H, $PCHMe_2$) ppm. $^{13}C\{^1H\}$ NMR ($CDCl_3$): δ = 98.1 (d, $^2J_{PC}$ = 11.0 Hz, CH of Ph), 95.9 (s, C_{ipso} of Ph), 95.3 and 81.5 (s, CH of Ph), 67.7 (s, OCH_2), 29.3 (s, CH_2Ph), 27.7 (d, $^1J_{PC}$ = 26.7 Hz, $PCHMe_2$), 18.5 and 16.6 (s, $PCHMe_2$) ppm. Elemental analysis calcd (%) for $C_{14}H_{23}Cl_2OPRu$: C 40.99, H 5.65; found: C 41.10, H 5.55. (**10c**):[16] Reaction time: 2 h (method A) or 1.5 h (method B). Yield: 0.030 g (72%) (method A) or 0.033 g (79%) (method B). $^{31}P\{^1H\}$ NMR ($CDCl_3$): δ = 156.3 (s) ppm. ^1H NMR (CD_2Cl_2): δ = 6.15 (t, 1H, $^3J_{HH}$ = 5.6 Hz, CH_{para} of Ph), 5.76 (t, 2H, $^3J_{HH}$ = 5.6 Hz, CH_{meta} of Ph), 5.54 (d, 2H, $^3J_{HH}$ = 5.6 Hz, CH_{ortho} of Ph), 4.32–4.24 (m, 2H, $^3J_{PH}$ = 13.8 Hz, $^3J_{HH}$ = 5.4 Hz, OCH_2), 3.05–2.97 (m, 2H, $PCHMe_2$), 2.77 (t, 2H, $^3J_{HH}$ = 6.0 Hz, CH_2Ph), 2.14–2.06 (m, 2H, CH_2), 1.31–1.16 (m, 12H, $PCHMe_2$) ppm. $^{13}C\{^1H\}$ NMR ($CDCl_3$): δ = 100.3 (d, $^2J_{PC}$ = 7.7 Hz, CH of Ph), 94.3 (s, C_{ipso} of Ph), 89.0 and 87.7 (s, CH of Ph), 64.7 (d, $^1J_{PC}$ = 3.6 Hz, OCH_2), 29.6 (d, $^1J_{PC}$ = 23.9 Hz, $PCHMe_2$), 29.4 and 25.1 (s, CH_2 and CH_2Ph), 18.8 (d, $^2J_{PC}$ = 2.6 Hz, $PCHMe_2$), 17.9 (s, $PCHMe_2$) ppm.

General procedure for the catalytic cross dehydrogenative coupling of hydrosilanes and alcohols using complex $[RuCl_2\{\eta^6{:}\kappa^1(P)\text{-}C_6H_5(CH_2)_3OP^iPr_2\}]$ (10c)

Under inert atmosphere, the corresponding hydrosilane (5 mmol), alcohol (1 mL) and complex **10c** (0.005–0.05 mmol; 0.1–1 mol%) were introduced in a Schlenk tube equipped with a bubbler, and the reaction mixture stirred at room temperature until complete conversion of the starting hydrosilane. The course of the reaction was monitored regularly taking samples of *ca.* 5 μL which, after dilution with CH_2Cl_2, were analyzed by GC. For the isolation of the alkoxysilane products, the reaction mixture was first subjected to a flash chromatography over silica gel, eluting with hexanes, and subsequently to vacuum-line evaporation or Kugelrohr distillation to eliminate all the volatiles. The identity of the alkoxysilanes was assessed by comparison of their NMR spectroscopic data with those reported in the literature (copies of the ^1H and $^{13}C\{^1H\}$ NMR spectra of the products obtained are included in the ESI file†).

X-ray crystal structure determination of compounds 6c and 10a–c

Crystals of **6c** and **10a,c** suitable for X-ray diffraction analysis were obtained by slow diffusion of *n*-hexane into a saturated solution of the complexes in tetrahydrofuran or dichloromethane, respectively. For **10b**, the crystals were obtained by slow diffusion of diethyl ether into a saturated solution of the complex in dichloromethane. The most relevant crystal and refinement data are collected in Table 3. In all the cases, data collection was performed with a Rigaku-Oxford Diffraction Xcalibur Onyx Nova single-crystal diffractometer using Cu-Kα radiation (λ = 1.5418 Å). Images were collected at a fixed crystal-to-detector distance of 62 mm using the oscillation method, with 1.20° oscillation and 4.5–11.0 s variable exposure time per image for **6c** and 30.0–130.0 s for **10c**. For **10a** and **10b**, the oscillation method was used with 1.10° oscillation, and 2.0–4.5 s or 7.5–17.0 s variable exposure time per image, respectively. Data collection strategy was calculated with the program CrysAlis^{Pro} CCD.[38] Data reduction and cell refinement were performed with the program CrysAlis^{Pro} RED.[38] An empirical absorption correction was applied using the SCALE3 ABSPACK algorithm as implemented in the program CrysAlis^{Pro} RED.[38] The software package WINGX was used for space group determination, structure solution, and refinement.[39] The structures were solved by Patterson interpretation and phase expansion using SIR92 (**6c** and **10a**)[40] or DIRDIF2008 (**10b** and **10c**).[41] Isotropic least-squares refinement on F^2 using SHELXL97 was performed.[42] During the final stages of the refinements, all the positional parameters and the anisotropic temperature factors of all non-H atoms were refined. All H atoms were geometrically located and their coordinates were refined riding on their parent atoms. The function minimized was $\{\sum[\omega(F_o^2 - F_c^2)^2]/\sum[\omega(F_o^2)^2]\}^{1/2}$ where $\omega = 1/[\sigma^2(F_o^2) + (aP)^2 + bP]$ (a and b values are given in Table 3) with $\sigma(F_o^2)$ from counting statistics and $P = [\max(F_o^2, 0) + 2F_c^2]/3$. Atomic scattering factors were taken from

Table 3 Crystal data and structure refinement for compounds **6c** and **10a–c**

	6c	**10a**	**10b**	**10c**
Empirical formula	$C_{25}H_{39}Cl_2OPRu$	$C_{13}H_{21}Cl_2OPRu$	$C_{14}H_{23}Cl_2OPRu$	$C_{15}H_{25}Cl_2OPRu$
Formula weight	558.50	396.24	410.26	424.29
Temperature/K	150(2)	150(2)	150(2)	293(2)
Wavelength/Å	1.54184	1.54184	1.54184	1.54184
Crystal system	Monoclinic	Triclinic	Orthorhombic	Orthorhombic
Space group	$P2_1/n$	$P\bar{1}$	*Pbca*	*Pbca*
Crystal size/mm	0.11 × 0.06 × 0.05	0.40 × 0.19 × 0.05	0.20 × 0.13 × 0.08	0.11 × 0.04 × 0.03
a/Å	9.3696(1)	7.2966(3)	8.8108(1)	8.9634(2)
b/Å	15.1236(2)	7.6884(3)	13.2483(2)	13.7539(3)
c/Å	18.3093(2)	15.4349(6)	27.2268(4)	27.5000(6)
α (°)	90	85.087(3)	90	90
β (°)	98.796(1)	81.257(4)	90	90
γ (°)	90	62.338(4)	90	90
Z	4	2	8	8
Volume/Å^3	2563.95(5)	757.89(6)	3178.13(8)	3390.2(2)
Calculated density/g cm^{-3}	1.447	1.736	1.715	1.663
μ/mm^{-1}	7.557	12.494	11.941	11.215
F(000)	1160	400	1664	1728
θ range/°	3.80–69.47	5.76–69.22	3.71–69.41	5.88–69.46
Index ranges	$-11 \le h \le 11$	$-7 \le h \le 8$	$-10 \le h \le 10$	$-8 \le h \le 10$
	$-17 \le k \le 18$	$-9 \le k \le 9$	$-15 \le k \le 15$	$-15 \le k \le 16$
	$-22 \le l \le 20$	$-18 \le l \le 18$	$-32 \le l \le 32$	$-33 \le l \le 31$
Completeness to θ_{max}	99.0%	99.6%	99.7%	99.9%
No. of reflns. collected	14 073	5736	10 246	9404
No. of unique reflns.	4781 (R_{int} = 0.0272)	2819 (R_{int} = 0.0613)	2953 (R_{int} = 0.0282)	3147 (R_{int} = 0.0318)
No. of parameters/restraints	278/0	167/0	176/0	181/0
Refinement method	Full-matrix least-squares on F^2			
Goodness-of-fit on F^2	1.030	1.059	1.044	1.118
Weight function (a, b)	0.0267, 0.0925	0.1116, 0.0000	0.0367, 1.6410	0.0570, 0.2256
R_1 [$I > 2\sigma(I)$][a]	0.0216	0.0504	0.0262	0.0302
wR_2 [$I > 2\sigma(I)$][a]	0.0507	0.1376	0.0647	0.0892
R_1 (all data)	0.0253	0.0517	0.0294	0.0324
R_2 (all data)	0.0527	0.1405	0.0672	0.0918
Largest diff. peak and hole/e Å^{-3}	0.287, −0.520	0.998, −1.790	0.575, −0.737	0.366, −0.753

[a] $R_1 = \sum(|F_o| - |F_c|)/\sum|F_o|$; $wR_2 = \{\sum[w(F_o^2 - F_c^2)^2]/\sum[w(F_o^2)^2]\}^{1/2}$.

International Tables for X-ray Crystallography, Volume C.[43] Geometrical calculations related to the centroids C* were made with PARST.[44] The crystallographic plots were made with DIAMOND.[45]

Conflicts of interest

There are no conflicts to declare.

Acknowledgements

Financial support from the Spanish Ministry of Economy, Industry and Competitiveness (MINECO project CTQ2016-75986-P) and the University of Oviedo (project PAPI-18-GR-2011-0032) is gratefully acknowledged. R. G.-F. thanks MECD of Spain for the award of a FPU fellowship (FPU17/00230).

Notes and references

1 G. Winkhaus and H. Singer, *J. Organomet. Chem.*, 1967, **7**, 487.

2 For review articles covering the chemistry of this type of compounds, see: (*a*) H. Le Bozec, D. Touchard and P. H. Dixneuf, *Adv. Organomet. Chem.*, 1989, **29**, 163; (*b*) M. A. Bennett, *Coord. Chem. Rev.*, 1997, **166**, 225; (*c*) F. C. Pigge and J. J. Coniglio, *Curr. Org. Chem.*, 2001, **5**, 757; (*d*) T. J. Geldbach and P. S. Pregosin, *Eur. J. Inorg. Chem.*, 2002, 1907; (*e*) E. P. Kündig, *Top. Organomet. Chem.*, 2004, **7**, 3; (*f*) B. Therrien, *Coord. Chem. Rev.*, 2009, **253**, 493; (*g*) S. K. Singh and D. S. Pandey, *RSC Adv.*, 2014, **4**, 1819; (*h*) G. Süss-Fink, *J. Organomet. Chem.*, 2014, **751**, 2.

3 For additional selected reviews covering the field, see: (*a*) L. Delaude and A. Demonceau, *Dalton Trans.*, 2012, **41**, 9257; (*b*) P. Crochet and V. Cadierno, *Dalton Trans.*, 2014, **43**, 12447; (*c*) P. Kumar, R. K. Gupta and D. S. Pandey, *Chem. Soc. Rev.*, 2014, **43**, 707; (*d*) L. Ackermann, *Org. Process Res. Dev.*, 2015, **19**, 260; (*e*) C. Bruneau and P. H. Dixneuf, *Top. Organomet. Chem.*, 2016, **55**, 137; (*f*) R. Manikandan and M. Jeganmohan, *Chem. Commun.*, 2017, **53**, 8931; (*g*) J. M. Gichumbi and H. B. Friedrich, *J. Organomet. Chem.*, 2018, **866**, 123.

4 For additional selected reviews covering the field, see: (*a*) Y. K. Yan, M. Melchart, A. Habtemariam and P. J. Sadler, *Chem. Commun.*, 2005, 4764; (*b*) G. Süss-Fink,

Dalton Trans., 2010, **39**, 1673; (*c*) G. S. Smith and B. Therrien, *Dalton Trans.*, 2011, **40**, 10793; (*d*) W. H. Ang, A. Casini, G. Sava and P. J. Dyson, *J. Organomet. Chem.*, 2011, **696**, 989; (*e*) A. A. Nazarov, C. G. Hartinger and P. J. Dyson, *J. Organomet. Chem.*, 2014, **751**, 251; (*f*) B. S. Murray, M. V. Babak, C. G. Hartinger and P. J. Dyson, *Coord. Chem. Rev.*, 2016, **306**, 86; (*g*) L. Zeng, P. Gupta, Y. Chen, E. Wang, L. Ji, H. Chao and Z.-S. Chen, *Chem. Soc. Rev.*, 2017, **46**, 5771; (*h*) M. Zaki, S. Hairat and E. S. Aazam, *RSC Adv.*, 2019, **9**, 3239.

5 For additional selected reviews covering the field, see: (*a*) K. Severin, *Chem. Commun.*, 2006, 3859; (*b*) B. Therrien, *Eur. J. Inorg. Chem.*, 2009, 2445; (*c*) A. Mishra, S. C. Kang and K.-W. Chi, *Eur. J. Inorg. Chem.*, 2013, 5222; (*d*) A. K. Singh, D. S. Pandey, Q. Xu and P. Braunstein, *Coord. Chem. Rev.*, 2014, **270–271**, 31; (*e*) B. Therrien, *CrystEngComm*, 2015, **17**, 484; (*f*) A. Bacchi and P. Pelagatti, *CrystEngComm*, 2016, **18**, 6114; (*g*) B. Therrien, *Adv. Inorg. Chem.*, 2018, **71**, 379.

6 For a general review on the chemistry of metal complexes with tethered arene ligands, see: J. R. Adams and M. A. Bennett, *Adv. Organomet. Chem.*, 2006, **54**, 293.

7 See, for example: M. Navarro, D. Vidal, P. Clavero, A. Grabulosa and G. Muller, *Organometallics*, 2015, **34**, 973 and references cited therein.

8 For representative examples, see: (*a*) B. Çetinkaya, S. Demir, I. Özdemir, L. Toupet, D. Sémeril, C. Bruneau and P. H. Dixneuf, *Chem. – Eur. J.*, 2003, **9**, 2323; (*b*) V. Cadierno, J. Díez, J. García-Álvarez and J. Gimeno, *Chem. Commun.*, 2004, 1820; (*c*) T. J. Geldbach, G. Laurenczy, R. Scopelliti and P. J. Dyson, *Organometallics*, 2006, **25**, 733; (*d*) I. Özdemir, S. Demir, B. Çetinkaya, L. Toupet, R. Castarlenas, C. Fischmeister and P. H. Dixneuf, *Eur. J. Inorg. Chem.*, 2007, 2862; (*e*) M. V. Baker, D. H. Brown, R. A. Haque, B. W. Skelton and A. H. White, *Dalton Trans.*, 2010, **39**, 70; (*f*) N. Kaloğlu, I. Özdemir, N. Gürbüz, H. Arslan and P. H. Dixneuf, *Molecules*, 2018, **23**, 647.

9 For representative examples, see: (*a*) B. Therrien and T. R. Ward, *Angew. Chem., Int. Ed.*, 1999, **38**, 405; (*b*) D. J. Morris, A. M. Hayes and M. Wills, *J. Org. Chem.*, 2006, **71**, 7035; (*c*) R. Hodgkinson, V. Jurčik, A. Zanotti-Gerosa, H. G. Nedden, A. Blackaby, G. J. Clarkson and M. Wills, *Organometallics*, 2014, **33**, 5517; (*d*) F. Martínez-Peña and A. M. Pizarro, *Chem. – Eur. J.*, 2017, **23**, 16231; (*e*) R. Soni, K. E. Jolley, S. Gosiewska, G. J. Clarkson, Z. Fang, T. H. Hall, B. N. Treloar, R. Knighton and M. Wills, *Organometallics*, 2018, **37**, 48; (*f*) T. J. Prior, H. Savoie, R. S. Boyle and B. S. Murray, *Organometallics*, 2018, **37**, 294.

10 For representative examples, see: (*a*) Y. Miyaki, T. Onishi, S. Ogoshi and H. Kurosawa, *J. Organomet. Chem.*, 2000, **616**, 135; (*b*) G. Marconi, H. Baier, F. W. Heinemman, P. Pinto, H. Pritzkow and U. Zenneck, *Inorg. Chim. Acta*, 2003, **352**, 188; (*c*) J. Čubrilo, I. Hartenbach, T. Schleid and R. F. Winter, *Z. Anorg. Allg. Chem.*, 2006, **632**, 400; (*d*) B. Lastra-Barreira, J. Díez, P. Crochet and I. Fernández, *Dalton Trans.*, 2013, **42**, 5412; (*e*) F. Martínez-Peña, S. Infante-Tadeo, A. Habtemariam and A. M. Pizarro, *Inorg. Chem.*, 2018, **57**, 5657; (*f*) B. Lastra-Barreira, J. Francos, P. Crochet and V. Cadierno, *Organometallics*, 2018, **37**, 3465.

11 For representative examples, see: (*a*) R. Y. C. Shin, G. K. Tan, L. L. Koh and L. Y. Goh, *Organometallics*, 2004, **23**, 6293; (*b*) Y. Ohki, Y. Takikawa, H. Sadohara, C. Kesenheimer, B. Engendahl, E. Kapatina and K. Tatsumi, *Chem. – Asian J.*, 2008, **3**, 1625; (*c*) T. Stahl, H. F. T. Klare and M. Oestreich, *J. Am. Chem. Soc.*, 2013, **135**, 1248; (*d*) T. Stahl, P. Hrobárik, C. D. F. Königs, Y. Ohki, K. Tatsumi, S. Kemper, M. Kaupp, H. F. T. Klare and M. Oestreich, *Chem. Sci.*, 2015, **6**, 4324; (*e*) S. Bähr, A. Simonneau, E. Irran and M. Oestreich, *Organometallics*, 2016, **35**, 925; (*f*) S. Wübbolt, M. S. Maji, E. Irran and M. Oestreich, *Chem. – Eur. J.*, 2017, **23**, 6213.

12 J. H. Nelson, K. Y. Ghebreyessus, V. C. Cook, A. J. Edwards, W. Wielandt, S. B. Wild and A. C. Willis, *Organometallics*, 2002, **21**, 1727.

13 See, for example: (*a*) M. A. Bennett and J. R. Harper, in *Modern Coordination Chemistry*, ed. G. J. Leigh and N. Winterton, RSC Publishing, Cambridge, 2002, pp. 163–168 and references cited therein; (*b*) J. W. Faller and D. G. D'Alliessi, *Organometallics*, 2003, **22**, 2749; (*c*) K. Umezawa-Vizzini and T. R. Lee, *Organometallics*, 2004, **23**, 1448; (*d*) J. W. Faller and P. P. Fontaine, *Organometallics*, 2005, **24**, 4132; (*e*) P. Pinto, A. W. Götz, G. Marconi, B. A. Hess, A. Marinetti, F. W. Heinemann and U. Zenneck, *Organometallics*, 2006, **25**, 2607; (*f*) R. Aznar, G. Muller, D. Sainz, M. Font-Bardia and X. Solans, *Organometallics*, 2008, **27**, 1967; (*g*) R. Aznar, A. Grabulosa, A. Mannu, G. Muller, D. Sainz, V. Moreno, M. Font-Bardia, T. Calvet and J. Lorenzo, *Organometallics*, 2013, **32**, 2344.

14 L. Weber, F. W. Heinemann, W. Bauer, S. Superchi, A. Zahl, D. Richter and U. Zenneck, *Organometallics*, 2008, **27**, 4116.

15 M. K. Pandey, J. T. Mague and M. S. Balakrishna, *Inorg. Chem.*, 2018, **57**, 7468.

16 Y. Miyaki, T. Onishi and H. Kurosawa, *Inorg. Chim. Acta*, 2000, **300–302**, 369.

17 Substitution reactions of one of the chloride ligands of complexes **A** and **C** by amines and CO, respectively, were also described. See ref. 14 and 16.

18 The tethered coordination of an arene-bis(pentafluorophenyl)phosphinite ligand to ruthenium was unsuccessfully attempted by Ward and co-workers: B. Therrien, T. R. Ward, M. Pilkington, C. Hoffmann, F. Gilardoni and J. Weber, *Organometallics*, 1998, **17**, 330.

19 (*a*) Igau and co-workers reported some examples of tethered arene-ruthenium(II) complexes containing *N*-phosphino amidine donors: D. Arquier, L. Vendier, K. Miqueu, J.-M. Sotiropoulos, S. Bastin and A. Igau, *Organometallics*, 2009, **28**, 4945; (*b*) An amino-phosphine analogue to **B** was also described by Balakrishna and co-workers in ref. 15.

20 (*a*) Although Kurosawa and co-workers originally referred to [$RuCl_2\{\eta^6{:}\kappa^1(O)\text{-}C_6H_5CH_2CH_2CH_2OH\}$] as a dimer, *i.e.* [$\{RuCl(\mu\text{-}Cl)(\eta^6\text{-}C_6H_5CH_2CH_2CH_2OH)\}_2$] (see ref. 16), its monomeric tethered structure was later established by Winter and co-workers through single-crystal X-ray diffraction studies (see ref. 10c); (*b*) The same approach had been previously employed for the preparation of compounds [$Cr(CO)_2\{\eta^6{:}\kappa^1(P)\text{-}C_6H_5(CH_2)_nOPPh_2\}$] ($n$ = 1, 2, 3) from [$Cr(CO)_3\{\eta^6\text{-}C_6H_5(CH_2)_nOH\}$]: W. R. Jackson, I. D. Rae and M. G. Wong, *Aust. J. Chem.*, 1984, **37**, 1563.

21 For a recent review article on the catalytic formation of silicon-heteroatom bonds, covering the cross dehydrogenative coupling of hydrosilanes with alcohols and highlighting the synthetic utility of the alkoxysilane products, see: K. Kuciński and G. Hreczycho, *ChemCatChem*, 2017, **9**, 1868.

22 (*a*) K. Masutani, T. Minowa, Y. Hagiwara and T. Mukaiyama, *Bull. Chem. Soc. Jpn.*, 2006, **79**, 1106; (*b*) T. Shintou, W. Kikuchi and T. Mukaiyama, *Bull. Chem. Soc. Jpn.*, 2003, **76**, 1645.

23 The only previous examples of metal complexes containing these ligands coordinated in a κ^1-(*P*) manner are [$Ni(Ph_2POCH_2Ph)_4$], *trans*-[$PdX_2(Ph_2POCH_2Ph)_2$] (X = Cl, CN) and *cis*-[$PdCl_2(Ph_2POCH_2Ph)(L)$] (L = $PhPMe_2$, $PhP(OMe)_2$): (*a*) A. W. Verstuyft and J. H. Nelson, *Synth. React. Inorg. Met.-Org. Chem.*, 1975, **5**, 69; (*b*) A. W. Verstuyft, D. A. Redfield, L. W. Cary and J. H. Nelson, *Inorg. Chem.*, 1976, **15**, 1128; (*c*) A. W. Verstuyft, L. W. Cary and J. H. Nelson, *Inorg. Chem.*, 1976, **15**, 3161; (*d*) C. W. Weston, A. W. Verstuyft, J. H. Nelson and H. B. Jonassen, *Inorg. Chem.*, 1977, **16**, 1313; (*e*) A. W. Verstuyft, D. A. Redfield, L. W. Cary and J. H. Nelson, *Inorg. Chem.*, 1977, **16**, 2776.

24 M. A. Bennett and A. K. Smith, *J. Chem. Soc., Dalton Trans.*, 1974, 233.

25 B. Choubey, P. S. Prasad, J. T. Mague and M. S. Balakrishna, *Eur. J. Inorg. Chem.*, 2018, 1707.

26 In toluene at 120 °C, minor amounts of complexes [$RuCl_2\{\eta^6{:}\kappa^1(P)\text{-}C_6H_5(CH_2)_nOPPh_2\}$] (**9a–c**) are also formed, along with species of type [$RuCl_2(\eta^6\text{-toluene})\{Ph_2PO(CH_2)_nPh\}$] resulting from the displacement of the *p*-cymene ligand by the toluene solvent.

27 E. L. Muetterties, J. R. Bleeke and A. C. Sievert, *J. Organomet. Chem.*, 1979, **178**, 197.

28 S. M. Hubig, S. V. Lindeman and J. K. Kochi, *Coord. Chem. Rev.*, 2000, **200–202**, 831.

29 P. E. Garrou, *Chem. Rev.*, 1981, **81**, 229.

30 For general reviews on catalytic dehydrocoupling processes, see: (*a*) F. Gauvin, J. F. Harrod and H. G. Woo, *Adv. Organomet. Chem.*, 1998, **42**, 363; (*b*) T. J. Clark, K. Lee and I. Manners, *Chem. – Eur. J.*, 2006, **12**, 8634; (*c*) R. Waterman, *Chem. Soc. Rev.*, 2013, **42**, 5629; (*d*) R. L. Melen, *Chem. Soc. Rev.*, 2016, **45**, 775.

31 See, for example: D. Ventura-Espinosa, S. Sabater, A. Carretero-Cerdán, M. Baya and J. A. Mata, *ACS Catal.*, 2018, **8**, 2558 and references cited therein.

32 See, for example: (*a*) S. V. Maifeld, R. L. Miller and D. Lee, *Tetrahedron Lett.*, 2002, **43**, 6363; (*b*) R. L. Miller, S. V. Maifeld and D. Lee, *Org. Lett.*, 2004, **6**, 2773; (*c*) Y. Ojima, K. Yamaguchi and N. Mizuno, *Adv. Synth. Catal.*, 2009, **351**, 1405; (*d*) D. V. Gutsulyak, S. F. Vyboishchikov and G. I. Nikonov, *J. Am. Chem. Soc.*, 2010, **132**, 5950; (*e*) C. K. Toh, H. T. Poh, C. S. Lim and W. Y. Fan, *J. Organomet. Chem.*, 2012, **717**, 9; (*f*) K. Kanno, Y. Aikawa and S. Kyushin, *Tetrahedron Lett.*, 2017, **58**, 9; (*g*) D. Ventura-Espinosa, A. Carretero-Cerdán, M. Baya, H. García and J. A. Mata, *Chem. – Eur. J.*, 2017, **23**, 10815; (*h*) J. Kaźmierczak, K. Kuciński, D. Lewandowski and G. Hreczycho, *Inorg. Chem.*, 2019, **58**, 1201.

33 Formation of this byproduct, arising from the presence of adventitious water, was previously observed by us while studying the same coupling reaction with platinum-based catalysts: J. Francos, J. Borge, S. Conejero and V. Cadierno, *Eur. J. Inorg. Chem.*, 2018, 3176.

34 Although we have not carried out mechanistic studies, we assume that the reaction proceeds through the same pathway proposed for [$RuCl_2(\eta^6\text{-}p\text{-cymene})(NHC)$] (**11**), in which the alcohol molecule attacks the silane once coordinated to the cationic fragment [$RuCl(\eta^6\text{-}p\text{-cymene})(NHC)$]$^+$ (see ref. 32g). According to this, the higher reactivity of the diisopropylphosphinite derivatives **10a–c** *vs.* their diphenylphosphinite counterparts **9a–c** is probably related to the greater electronic density of the metal center in the former, which facilitates the dissociation of one of the chloride ligands.

35 For comparative purposes we performed the same reaction employing 0.01 mol% of the non-tethered derivative [$RuCl_2(\eta^6\text{-benzene})\{Ph_2PO(CH_2)_3Ph\}$] (**7c**). It also showed a good catalytic activity, but its effectiveness was lower than that of [$RuCl_2\{\eta^6{:}\kappa^1(P)\text{-}C_6H_5(CH_2)_3OPPh_2\}$] (**9c**) (130 min were needed to attain the complete conversion of the starting silane; to be compared with entry 9 in Table 2). This result points to a positive effect of the tethered structure on the catalytic activity. In addition, we also carry out the reaction using the known complex [$RuCl_2(\eta^6\text{-}p\text{-cymene})(PPh_3)$] as catalyst (0.01 mol%). After 2 h at r.t., only 5% conversion was observed, indicating that the nature of the *P*-donor ligand (phosphinite *vs.* phosphine) exerts a strong effect on this catalytic transformation.

36 Ruthenium(II) complexes are known to react with terminal propargylic alcohols to generate allenylidene or vinylidene-type complexes. See, for example: (*a*) M. I. Bruce, *Chem. Rev.*, 1998, **98**, 2797; (*b*) V. Cadierno and J. Gimeno, *Chem. Rev.*, 2009, **109**, 3512.

37 W. L. F. Armarego and C. L. L. Chai, in *Purification of Laboratory Chemicals*, Butterworth-Heinemann, Oxford, U. K., 5th edn, 2003.

38 *CrysAlisPro CCD & CrysAlisPro RED*, Oxford Diffraction Ltd., Oxford, U.K., 2008.

39 L. J. Farrugia, *J. Appl. Crystallogr.*, 2012, **45**, 849.

40 A. Altomare, G. Cascarano, C. Giacovazzo and A. Gualardi, *J. Appl. Crystallogr.*, 1993, **26**, 343.

41 P. T. Beurskens, G. Beurskens, R. de Gelder, S. García-Granda, R. O. Gould and J. M. M. Smits, *DIRDIF2008 program system. Crystallography Laboratory*, University of Nijmegen, Nijmegen, The Netherlands, 2008.
42 G. M. Sheldrick, *SHELXL97: Program for the Refinement of Crystal Structures*, University of Göttingen, Göttingen, Germany, 1997.
43 *International Tables for X-Ray Crystallography, Volume C*, ed. A. J. C. Wilson, Kluwer Academic Publishers, Dordrecht, The Netherlands, 1992.
44 M. Nardelli, *Comput. Chem.*, 1983, **7**, 95.
45 K. Brandenburg and H. Putz, *DIAMOND, Crystal Impact GbR*, Bonn, Germany, 1999.